

ANALYSIS OF RECONSTRUCTION FROM NOISY DISCRETE GENERALIZED RADON DATA

ALEXANDER KATSEVICH¹

ABSTRACT. We consider a wide class of generalized Radon transforms \mathcal{R} , which act in \mathbb{R}^n for any $n \geq 2$ and integrate over submanifolds of any codimension N , $1 \leq N \leq n - 1$. Also, we allow for a fairly general reconstruction operator \mathcal{A} . The main requirement is that \mathcal{A} be a Fourier integral operator with a phase function, which is linear in the phase variable. We consider the task of image reconstruction from discrete data $g_{j,k} = (\mathcal{R}f)_{j,k} + \eta_{j,k}$. We show that the reconstruction error $N_\epsilon^{\text{rec}} = \mathcal{A}\eta_{j,k}$ satisfies $N^{\text{rec}}(\tilde{x}; x_0) = \lim_{\epsilon \rightarrow 0} N_\epsilon^{\text{rec}}(x_0 + \epsilon\tilde{x})$, $\tilde{x} \in D$. Here x_0 is a fixed point, $D \subset \mathbb{R}^n$ is a bounded domain, and $\eta_{j,k}$ are independent, but not necessarily identically distributed, random variables. N^{rec} and N_ϵ^{rec} are viewed as continuous random functions of the argument \tilde{x} (random fields), and the limit is understood in the sense of probability distributions. Under some conditions on the first three moments of $\eta_{j,k}$ (and some other not very restrictive conditions on x_0 and \mathcal{A}), we prove that N^{rec} is a zero mean Gaussian random field and explicitly compute its covariance. We also present a numerical experiment with a cone beam transform in \mathbb{R}^3 , which shows an excellent match between theoretical predictions and simulated reconstructions.

1. INTRODUCTION

1.1. Prior work. Main results. Tomographic imaging, which includes X-ray, ultrasound, seismic, and many other tomographies, is commonly used in a wide range of applications such as medical, industrial, security, and others. The task of tomographic image reconstruction can be formulated as follows. Let $\mathcal{R} : \mathcal{X} \rightarrow \mathcal{V}$ denote a linear integral transform, where $\mathcal{X} \subset \mathbb{R}^n$ is the image domain and $\mathcal{V} \subset \mathbb{R}^n$ is the data domain. Let f be a function supported in \mathcal{X} , which represents the object being scanned. Tomographic data represent integrals of f along a family of manifolds (e.g., lines, spheres, etc.). The manifolds are parametrized by points $\omega \in \mathcal{V}$, so the data are $(\mathcal{R}f)(\omega)$, $\omega \in \mathcal{V}$. In a continuous setting, the goal is to reconstruct $f(x)$, $x \in \mathcal{X}$ (or some information about f , e.g., its singularities) from $(\mathcal{R}f)(\omega)$, $\omega \in \mathcal{V}$.

In practice, data are always discrete and contain noise. So the task becomes to reconstruct an approximation to f from discrete data $g_j := (\mathcal{R}f)(\epsilon j) + \eta_j$, $\epsilon j \in \mathcal{V}$, $j \in \mathbb{Z}^n$. Here $\epsilon > 0$ represents the data step size and η_j 's represent additive noise. For simplicity, we assume that the step size is the same along each direction. Usually, two most important factors that affect quality of reconstructed images are data discretization and strength of noise in the data.

¹This work was supported in part by NSF grant DMS-1906361. Department of Mathematics, University of Central Florida, Orlando, FL 32816 (Alexander.Katsevich@ucf.edu).

Effects of data discretization on various aspects of image quality, e. g. spatial resolution, aliasing artifacts, are now well-understood [14, 33, 34, 40]. In particular, in a series of articles, the author developed an approach, called *local reconstruction analysis* (LRA), to analyze the resolution with which the singularities (i.e., jump discontinuities) of f are reconstructed from discrete tomographic data in the absence of noise, see [20, 22, 23] and references therein. In those articles the singularities of f are assumed to lie on a smooth curve in \mathbb{R}^2 (and surface in \mathbb{R}^n) or a rough curve in \mathbb{R}^2 , denoted \mathcal{S} . In [24], LRA theory was advanced to include analysis of aliasing (ripple artifacts) in \mathbb{R}^2 at points away from \mathcal{S} .

The main idea of LRA is to obtain a simple formula to accurately approximate an image reconstructed from discrete data, f_ϵ^{rec} , in an ϵ -neighborhood of a point, x_0 . For example, let f be a real-valued function in \mathbb{R}^2 , $\mathcal{S} \subset \mathbb{R}^2$ be a smooth curve, and f have a jump across \mathcal{S} . Let f_ϵ^{rec} be a filtered backprojection (FBP) reconstruction of f from discretely sampled Radon transform (RT) data with sampling step size, ϵ . Under some mild conditions on \mathcal{S} , it is shown in [21, 23] that one has

$$(1.1) \quad \lim_{\epsilon \rightarrow 0} f_\epsilon^{\text{rec}}(x_0 + \epsilon \check{x}) = \Delta f(x_0) \text{DTB}(\check{x}; x_0), \quad x_0 \in \mathcal{S},$$

where the limit is uniform with respect to $\check{x} \in D$ for any bounded set D . Here $\Delta f(x_0)$ is the value of the jump of f across \mathcal{S} at x_0 and DTB, which stands for the *Discrete Transition Behavior*, is an easily computable function independent of f . The DTB function depends only on the curvature of \mathcal{S} at x_0 . When ϵ is sufficiently small, the right-hand side of (1.1) is an accurate approximation of f_ϵ^{rec} and the DTB function describes accurately the smoothing of the singularities of f in f_ϵ^{rec} .

As is seen from (1.1), *LRA provides a uniform approximation to $f_\epsilon^{\text{rec}}(x)$ in domains of size $\sim \epsilon$, which is of the same order of magnitude as the sampling step size ϵ .* Given the DTB function, one can study local properties of reconstruction from discrete data, such as spatial resolution and strength of artifacts.

The first extension of LRA to reconstruction from noisy data has been done in [2]. The authors consider the model $g = \mathcal{R}f + \eta$, where \mathcal{R} is the classical 2D RT, $\mathcal{R}f$ is the measured sinogram with entries $(\mathcal{R}f)_{j,k}$, and η is the noise. The entries, $\eta_{j,k}$, of η are assumed to be independent, but not necessarily identically distributed. Due to linearity of \mathcal{R}^{-1} , the reconstruction error is $\mathcal{R}^{-1}\eta$. Let $N_\epsilon^{\text{rec}}(x)$ denote the reconstruction error, i.e. the FBP reconstruction only from $\eta_{j,k}$. Similarly to previous works on LRA (cf. also (1.1)), the authors consider $O(\epsilon)$ -sized neighborhoods around any $x_0 \in \mathbb{R}^2$. Let $C(D)$ be the space of continuous functions on D , where $D \subset \mathbb{R}^2$ is a bounded domain. The main result of [2] is that, under suitable assumptions on the first three moments of the $\eta_{j,k}$, the boundary of D , and x_0 , the following limit exists:

$$(1.2) \quad N^{\text{rec}}(\check{x}; x_0) = \lim_{\epsilon \rightarrow 0} N_\epsilon^{\text{rec}}(x_0 + \epsilon \check{x}), \quad \check{x} \in D.$$

Here, N^{rec} and N_ϵ^{rec} are viewed as $C(D)$ -valued random variables (random fields), and the limit is understood in the sense of probability distributions. It is proven also that $N^{\text{rec}}(\check{x}; x_0)$ is a zero mean Gaussian random field

(GRF) and its covariance is computed explicitly. The paper also contains numerical experiments, which show an excellent match between theoretical predictions and simulated reconstructions.

In this paper we extend the results of [2] to a wide class of generalized RTs \mathcal{R} , which act in \mathbb{R}^n for any $n \geq 2$ and integrate over submanifolds of any codimension N , $1 \leq N \leq n - 1$. Also, we allow for a fairly general reconstruction operator \mathcal{A} . The main requirement is that \mathcal{A} be a Fourier integral operator (FIO) with a phase function, which is linear in the phase variable. Similarly to [2] we consider the model $g = \mathcal{R}f + \eta$ and show that the reconstruction error $N_\epsilon^{\text{rec}} = \mathcal{A}\eta_{j,k}$ satisfies (1.2), where $D \subset \mathbb{R}^n$ is a bounded domain and $\eta_{j,k}$ are independent, but not necessarily identically distributed, random variables. As in [2], N^{rec} and N_ϵ^{rec} are viewed as $C(D)$ -valued random variables, and the limit is understood in the sense of probability distributions. We prove that N^{rec} is a zero mean GRF and explicitly compute its covariance. We also present a numerical experiment with a cone beam transform in \mathbb{R}^3 , which shows an excellent match between theoretical predictions and simulated reconstructions.

1.2. Significance. Equations (1.1) and (1.2) together provide an explicit and accurate local approximation to the image reconstructed from noisy discrete data, $f_\epsilon^{\text{rec}} = \mathcal{A}(\mathcal{R}f + \eta)$. Eq. (1.1) describes the effect of edge smoothing due to data discretization, and (1.2) describes the reconstruction error due to random noise. The combined approximation is uniform over domains of size $\sim \epsilon$, i.e. precisely at the scale of *native* resolution enabled by available data. Results of this kind are more useful for localized analysis of tomographic reconstruction than more common global analyses, which estimate some global error norm (e.g., L^2). Formulas provided by LRA, such as (1.1) and (1.2), can be used to study resolution of reconstruction, perform statistical inference about detectability of small details in a reconstructed image, and for many other tasks.

As a first example we consider the task of detection and assessment of lung tumors in CT images (see also [2]). Typically, malignant lung tumors have rougher boundaries than benign nodules [10, 11]. Therefore the roughness of the nodule boundary is a critical factor for accurate diagnosis. Reconstructions from discrete X-ray CT data produce images in which the singularities are smoothed to various degrees. A rough boundary of the tumor may appear smoother in the reconstructed image than it really is. This can lead to a cancerous tumor being misdiagnosed as a benign nodule. Likewise, due to the random noise in the data, the smooth boundary of a benign nodule may appear rougher than it actually is, which may again result in misdiagnosis. This example illustrates the need to accurately quantify the effects of both data discretization and random noise on *local* (i.e., near the tumor boundary) tomographic reconstruction.

Another example is the use of CT by the energy industry for imaging of rock samples extracted from wells. The reconstructed image is segmented to identify as accurately as possible the pore space (i.e., voids) inside the sample. This is very challenging, because pore boundaries are fractal, they possess features that are below the scanner native resolution. Then one uses numerical fluid flow simulations *inside the identified pore space* to compute

permeability of the sample [5]. The obtained results are used for formation evaluation and improving of oil recovery [36]. Thus, the key step that affects the accuracy of the entire workflow from scanning to fluid flow simulation is CT image segmentation. Errors in locating pore boundaries and, consequently, inaccurate pore space identification lead to incorrect flow simulation and errors in computed permeability [9,37,38]. Therefore, as in the previous example, precise quantification of the local (near the boundaries) effects of data discretization and noise on the reconstructed image is of paramount importance.

1.3. Related literature. Organization of the paper. We now discuss related existing literature concerning reconstruction in a stochastic setting and compare it with our findings. A kernel-type estimator of f has been derived in [26,27] in the setting of a tomography problem with additive random errors in observations. Its minimax optimal rate of convergence to f , i.e. the ground truth function, has been established both at a fixed point and in a global L^2 norm. The rate of convergence for the maximal deviation of an estimator from its mean has been obtained for similar kernel-type estimators in [6]. The accuracy of pointwise asymptotically efficient kernel estimator in terms of minimax risk of a probability density f from noise-free RT data sampled on a random grid has been derived in [7,8].

An essential common feature of all the works cited above is that convergence is established by incorporating into the reconstruction/estimation algorithm of additional smoothing at a scale δ significantly larger than the data step size. This smoothing leads to a notable loss of resolution in practical applications. This is also the reason why the cited works assume that the function f being estimated is sufficiently smooth. To compare with our results, we mention two points. First, none of these papers obtain the probability distribution of the reconstructed noise (i.e., the error in the reconstruction), either pointwise or in a domain. Second, our reconstruction is performed and investigated at *native* resolution.

Reconstruction in the framework of Bayesian inversion has been explored as well [32,39,43]. Global inversion in the case when continuous data are corrupted by a Gaussian white noise is investigated in [32]. Using a Gaussian prior (i.e., with Tikhonov regularization), the authors establish the asymptotic normality of the posterior distribution and of the MAP estimator for observables of the kind $\int f(x)\psi(x)dx$, where $\psi \in C^\infty$ is a test function. This means that reconstruction is investigated at the scales ~ 1 . In contrast, our results quantify the pointwise reconstruction error uniformly over regions of size $O(\epsilon)$. Various other aspects of Bayesian inversion are discussed in [39,43].

Analysis of reconstruction errors using semiclassical analysis is developed in [41]. The goal of the paper is to analyze empirical spatial mean and variance of the noise in the inversion for a single experiment in the limit as the sampling rate ϵ goes to zero. In contrast, the emphasis of our paper is on the study of the reconstruction error across multiple reconstructions. We obtain the entire probability density function (PDF) of the error in the limit as $\epsilon \rightarrow 0$ (as opposed to only the mean and variance).

Analysis of noise in reconstructed images is an active area in more applied research as well (see [12, 44] and references therein). In this research, the proposed methodologies mostly combine numerical and semi-empirical approaches. Theoretical derivation of the reconstructed noise PDF in small neighborhoods is not provided.

The paper is organized as follows. In section 2, we describe the setting of the problem and main assumptions. In section 3, we state the main results, which are broken down into three theorems. In section 4 we illustrate how to check the key assumptions for a few common CT geometries. The beginning of the proof of the first result, theorem 3.1, is in section 5. In this section we study the contribution of the leading order term of \mathcal{A} to the reconstructed image, $N_\epsilon^{\text{rec}}(x_0 + \epsilon\check{x})$. In section 6 we study the contribution of the lower order terms of \mathcal{A} to the reconstruction. In section 7 we finish the proof of theorem 3.1 and prove theorem 3.2, our second main result. In section 8 we prove our last result, theorem 3.4. A numerical experiment is described in section 9. Finally, the proofs of some auxiliary lemmas are in Appendices A–E.

2. SETTING OF THE PROBLEM AND MAIN ASSUMPTIONS

A general Radon-type integral transform $\mathcal{R} : \mathcal{X} \rightarrow \mathcal{V}$, where $\mathcal{X}, \mathcal{V} \subset \mathbb{R}^n$ are some domains, can be written as a Fourier Integral Operator (FIO) with a phase function, which is linear in the frequency variable. Except for a small number of special cases, exact inversion formulas are usually not available. Hence one may be interested in applying an approximate inversion formula in the form of a parametrix. In other cases, one may be interested in enhanced-edge reconstruction [15, 18, 30, 35]. Therefore we consider a general reconstruction operator $\mathcal{A} : \mathcal{V} \rightarrow \mathcal{X}$, which is also an FIO with a linear phase function

$$(2.1) \quad (\mathcal{A}g)(x) = (2\pi)^{-N} \int_{\mathbb{R}^N} \int_{\mathcal{Y}} \int_{\mathcal{Z}} a(x, (y, z), \xi) e^{i\xi \cdot \Phi(x, (y, z))} g(y, z) dz dy d\xi.$$

where $\Phi : \mathcal{X} \times \mathcal{V} \rightarrow \mathbb{R}^N$ is a smooth function.

Assumption 2.1 (Properties of the domains \mathcal{X} , \mathcal{V}).

- (1) $\mathcal{X} \subset \mathbb{R}^n$ and $\mathcal{V} \subset \mathbb{R}^n$ are bounded domains.
- (2) $\mathcal{V} = \mathcal{Y} \times \mathcal{Z}$ for some domains $\mathcal{Y} \subset \mathbb{R}^{n-N}$, $\mathcal{Z} \subset \mathbb{R}^N$.

In our setting, $x \in \mathcal{X}$ are points in the image domain, and $(y, z) \in \mathcal{V}$ are points in the data (projection) domain. The pair $(y, z) \in \mathcal{V}$ was denoted ω in the Introduction. The representation of ω , $\omega = (y, z)$, as a pair is analogous to the classical RT convention $(\alpha, p) \in S^{n-1} \times \mathbb{R}$. In our case, y is the analog of the variable α and z is a (multidimensional) analog of the variable p .

Denote $\mathbb{N}_0 := \mathbb{N} \cup \{0\}$. For convenience, throughout the paper we use the following convention. If a constant c is used in an equation or inequality, the qualifier ‘for some $c > 0$ ’ is assumed. If several c are used in a string of (in)equalities, then ‘for some’ applies to each of them, and the values of different c ’s may all be different.

Definition 2.2. Pick any $\gamma \in \mathbb{R}$. The set $S^\gamma(\mathcal{X} \times \mathcal{V} \times (\mathbb{R}^N \setminus 0))$ is the vector space of all functions $a(x, \omega, \xi) : \mathcal{X} \times \mathcal{V} \times \mathbb{R}^N \rightarrow \mathbb{R}$ such that

$$(2.2) \quad \begin{aligned} & |\partial_\xi^m \partial_{(x,\omega)}^k a(x, \omega, \xi)| \leq c_{m,k} (1 + |\xi|)^{\gamma - |m|}, \\ & (x, \omega) \in \mathcal{X} \times \mathcal{V}, |\xi| \geq 1, m \in \mathbb{N}_0^N, k \in \mathbb{N}_0^{2n}; \\ & \partial_{(x,\omega)}^k a \in L_{loc}^1(\mathcal{X} \times \mathcal{V} \times \mathbb{R}^N), k \in \mathbb{N}_0^{2n}. \end{aligned}$$

Assumption 2.3 (Properties of a , the amplitude of \mathcal{A}).

(1) One has

$$(2.3) \quad a \in S^\gamma(\mathcal{X} \times \mathcal{V} \times (\mathbb{R}^N \setminus 0)) \text{ for some } \gamma > -N/2.$$

(2) The principal symbol of \mathcal{A} , denoted a_0 , is homogeneous and satisfies:

$$(2.4) \quad \begin{aligned} & a_0(x, \omega, r\xi) = r^\gamma a_0(x, \omega, \xi), r > 0, (x, \omega) \in \mathcal{X} \times \mathcal{V}, \xi \in \mathbb{R}^N \setminus 0, \\ & a_0 \in S^\gamma(\mathcal{X} \times \mathcal{V} \times (\mathbb{R}^N \setminus 0)). \end{aligned}$$

(3) $a - a_0 \in S^{\gamma'}(\mathcal{X} \times \mathcal{V} \times (\mathbb{R}^N \setminus 0))$ for some $\gamma' < \gamma$.

Assumption 2.4 (Properties of Φ).

(1) $\Phi : U \rightarrow \mathbb{R}^N$ is a smooth function, where $U \subset \mathbb{R}^{2n}$ is a neighborhood of $\mathcal{X} \times \mathcal{V}$.

(2) For each $x \in \mathcal{X}$ and $y \in \mathcal{Y}$ there exists a unique point $z = \Psi(x, y) \in \mathcal{Z}$ such that $\Phi(x, (y, \Psi(x, y))) \equiv 0$.

(3) $|\det(\partial_z \Phi(x, (y, z)))| \geq c > 0$ for any $z = \Psi(x, y)$ and $(x, y) \in \mathcal{X} \times \mathcal{Y}$.

Denote $u := (x, y)$, $a_0(u, z, \xi) := a_0(x, (y, z), \xi)$, and similarly for all other functions which depend on x and y . Assumption 2.4 and the implicit function theorem [28, Theorem 3.3.1] imply

(1) The function $z = \Psi(x, y) = \Psi(u)$, $u \in \mathcal{X} \times \mathcal{Y}$, is smooth.

(2) The equation $w = \Phi(u, z)$ can be solved for z and the solution $z(w, u)$ is smooth on the domain $[-\delta, \delta] \times (\mathcal{X} \times \mathcal{Y})$, where $\delta > 0$ is sufficiently small.

In the proof of the second statement we patch together local solutions similarly to [17, §8, exercise 14].

Define the set

$$(2.5) \quad \Lambda := \{(u, z) \in \mathcal{X} \times \mathcal{V} : z = z(w, u), |w| < \delta\}.$$

Thus Λ is a small neighborhood of the set $\{(u, z) \in \mathcal{X} \times \mathcal{V} : z = \Psi(u)\}$. Further, define the $N \times N$ matrix function

$$(2.6) \quad Q(u) := \partial_z \Phi(u, z)|_{z=\Psi(u)}, u \in \mathcal{X} \times \mathcal{Y}.$$

By assumption 2.4(3), $|\det Q(u)| \geq c > 0$ if $u \in \mathcal{X} \times \mathcal{Y}$. Differentiating the identity $\Phi(u, z(w, u)) \equiv w$ with respect to w we see that

$$(2.7) \quad z(w, u) = \Psi(u) + Q^{-1}(u)w + O(|w|^2), |w| \leq \delta, u \in \mathcal{X} \times \mathcal{Y}.$$

We suppose that $\delta > 0$ (and the set Λ) is sufficiently small so that

$$(2.8) \quad \|\partial_w^m z(w, u)\| \leq c_m, |\det(\partial_w z(w, u))| \geq c, m \in \mathbb{N}_0^N, |w| \leq \delta, u \in \mathcal{X} \times \mathcal{Y},$$

where $\|\cdot\|$ denotes any matrix norm.

One is given discrete data

$$(2.9) \quad \begin{aligned} g(y_j, z_k), \quad y_j = \epsilon_y j \in \mathcal{Y}, \quad j \in \mathbb{Z}^{n-N}, \quad z_k = \epsilon k \in \mathcal{Z}, \quad k \in \mathbb{Z}^N, \\ \epsilon/\epsilon_y \equiv \text{const}. \end{aligned}$$

Realistic data are usually represented as the sum of a useful signal (the RT of some function) and noise. The reconstruction operator \mathcal{A} is linear, so we assume that the useful signal is zero and the data consist only of noise: $g(y_j, z_k) = \eta_{j,k}$.

Assumption 2.5 (Properties of noise $\eta_{j,k}$).

- (1) $\eta_{j,k}$ are independent (but not necessarily identically distributed) random variables,
- (2) One has

$$(2.10) \quad \mathbb{E}\eta_{j,k}^2 = \epsilon^{2\gamma}\epsilon_y^{-(n-N)}\sigma^2(y_j, z_k), \quad \mathbb{E}|\eta_{j,k}|^3 = o(\epsilon^{3\gamma}\epsilon_y^{-2(n-N)}),$$

where $\sigma(y, z)$ is a Lipschitz continuous, bounded function on \mathcal{V} , and the small- o term is uniform in j, k as $\epsilon \rightarrow 0$.

Reconstruction is computed using the well-known filtered backprojection scheme.

- (1) Interpolate and, possibly, smooth the data along the z variable:

$$(2.11) \quad g_{\text{cont}}(y, z) := \sum_{z_k \in \mathcal{Z}} \varphi\left(\frac{z - z_k}{\epsilon}\right) g(y, z_k), \quad y = y_j \in \mathcal{Y}.$$

Here, φ is a compactly supported and sufficiently smooth function, which describes the effects of numerical interpolation and smoothing of the data.

- (2) Filtering step. Compute

$$(2.12) \quad \begin{aligned} N_\epsilon^{(1)}(x, y) &= (2\pi)^{-N} \int_{\mathbb{R}^N} \int_{\mathcal{Z}} a(x, (y, z), \xi) e^{i\xi \cdot \Phi(x, (y, z))} g_{\text{cont}}(y, z) dz d\xi, \\ y &= y_j \in \mathcal{Y}. \end{aligned}$$

- (3) Backprojection step. Compute the Riemann sum

$$(2.13) \quad N_\epsilon^{\text{rec}}(x) = \epsilon_y^{n-N} \sum_{y_j \in \mathcal{Y}} N_\epsilon^{(1)}(x, y_j).$$

For a domain $U \subset \mathbb{R}^n$, $n = 1, 2, \dots$, the notation $f \in C^k(\bar{U})$ means that $f(x)$ is k times differentiable up to the boundary and $\partial_x^m f \in L^\infty(U)$ for any multi-index m , $|m| \leq k$. The notation $f \in C_0^k(U)$ means that $f \in C^k(\bar{U})$ and $\text{supp}(f) \subset U$.

Assumption 2.6 (Properties of the kernel φ).

- (1) $\varphi \in C_0^M(\mathcal{Z})$ for some integer $M > \max(N + \gamma + 1, n/2)$.

Assumptions 2.3(1), 2.4(3), and 2.6(1) imply that the oscillatory integral (2.12) is well-defined.

We need the following technical definition.

Definition 2.7. [13, Chapter 2] Let F be any non-empty bounded subset of \mathbb{R}^n and let $N_\delta(F)$ be the smallest number of sets of diameter at most δ which can cover F . The *upper box-counting dimension* of F is defined as

$$(2.14) \quad \overline{\dim}_B(F) := \limsup_{\delta \rightarrow 0} \frac{\log(N_\delta(F))}{-\log(\delta)}.$$

An easier, but equivalent, definition is obtained by replacing $N_\delta(F)$ in (2.14) with $N'_\delta(F)$, which is the number of cubes of the form $\delta[m, m + \vec{1}]$, $m \in \mathbb{Z}^n$, intersecting F [13, Chapter 2]. Here $\vec{1} = (1, \dots, 1) \in \mathbb{Z}^n$.

Later on, we consider reconstruction in an ϵ -neighborhood of a point x_0 , which satisfies the following properties:

Assumption 2.8 (Properties of x_0).

- (1) For each $\xi \in \mathbb{R}^N \setminus 0$, the set

$$(2.15) \quad Y_1(x_0, \xi) := \{y \in \mathcal{Y} : \det(\partial_y^2(\xi \cdot \Psi(x_0, y))) = 0\}$$

has the upper box-counting dimension $\overline{\dim}_B(Y_1(x_0, \xi)) < n - N$.

- (2) There exist an open set $V \in \mathcal{Y}$ and an open cone $\Xi \subset \mathbb{R}^N \setminus 0$ such that

$$(2.16) \quad \begin{aligned} a_0(x_0, (y, \Psi(x_0, y)), \xi) &\neq 0, \quad \forall y \in V, \xi \in \Xi, \\ \sigma(y, \Psi(x_0, y)) &\neq 0, \quad \forall y \in V. \end{aligned}$$

- (3) For any $\tilde{x} \in \mathbb{R}^n \setminus 0$, the set

$$(2.17) \quad Y_2(x_0, \tilde{x}) := \{y \in \mathcal{Y} : \partial_x \Psi(x_0, y) \tilde{x} = 0\}$$

has Lebesgue measure zero.

For all practical purposes, we can think of Assumption 2.8(1) as saying that for each $\xi \in \mathbb{R}^N \setminus 0$, the set of points $y \in \mathcal{Y}$ such that the Hessian of the function $y \rightarrow \xi \cdot \Psi(x_0, y)$ is degenerate is locally a submanifold of codimension ≥ 1 . This assumption makes sense because the solution set of a generic scalar equation $f(y) = 0$, $y \in \mathcal{Y}$, is a surface of codimension 1.

Assumption 2.8(3) can be viewed as a consequence of a local Bolker condition. In terms of Ψ , the incidence relation defined by the generalized RT \mathcal{R} can be written in the form $z - \Psi(x, y) = 0$. In this case, the conventional global Bolker condition becomes $\partial_y \Psi(x_1, y) \neq \partial_y \Psi(x_2, y)$ for any $x_1, x_2 \in \mathcal{X}$, $x_1 \neq x_2$, and $y \in \mathcal{Y}$. Localizing to a neighborhood of some $x_0 \in \mathcal{X}$, we get

$$(2.18) \quad \partial_y[\Psi(x_0 + t\tilde{x}, y) - \Psi(x_0, y)] \neq 0, \quad 0 < |t| \ll 1.$$

Dividing by t and taking the limit as $t \rightarrow 0$ suggests the local condition

$$(2.19) \quad \partial_y \partial_x \Psi(x_0, y) \tilde{x} \neq 0 \quad \forall \tilde{x} \in \mathbb{R}^n \setminus 0, y \in \mathcal{Y}.$$

Note that the first zero in (2.19) stands for a $N \times (n - N)$ zero matrix. If (2.19) holds, then (2.17) holds as well. Equations (2.18) and (2.19) explain the intuition on which the condition (2.17) is based.

3. MAIN RESULTS

Theorem 3.1. *Let $x_0 \in \mathcal{X}$, $\tilde{x} \in \mathbb{R}^n$ be two fixed points. Suppose the domains \mathcal{X}, \mathcal{V} satisfy Assumption 2.1, the operator \mathcal{A} satisfies Assumption 2.3 and Assumption 2.4, the random variables $\eta_{k,j}$ satisfy Assumption 2.5, the kernel φ satisfies Assumption 2.6, and the point x_0 satisfies Assumption 2.8. One has*

$$(3.1) \quad N^{\text{rec}} := \lim_{\epsilon \rightarrow 0} N_{\epsilon}^{\text{rec}}(x_0 + \epsilon \tilde{x})$$

is a Gaussian random variable, and the limit is in the sense of distributions.

Let us choose $L \geq 1$ points $\tilde{x}_1, \dots, \tilde{x}_L \in \mathbb{R}^n$. The corresponding reconstructed vector is $\vec{N}_{\epsilon}^{\text{rec}} := (N_{\epsilon}^{\text{rec}}(x_0 + \epsilon \tilde{x}_1), \dots, N_{\epsilon}^{\text{rec}}(x_0 + \epsilon \tilde{x}_L)) \in \mathbb{R}^L$. For simplicity, the dependence of N^{rec} and $\vec{N}_{\epsilon}^{\text{rec}}$ on x_0 and \tilde{x} is suppressed from notation.

Theorem 3.2. *Let $x_0 \in \mathcal{X}$ and $\tilde{x}_l \in \mathbb{R}^n$, $l = 1, 2, \dots, L$, be fixed. Suppose the assumptions of Theorem 3.1 are satisfied. One has*

$$(3.2) \quad \vec{N}^{\text{rec}} := \lim_{\epsilon \rightarrow 0} \vec{N}_{\epsilon}^{\text{rec}}(x_0 + \epsilon \tilde{x})$$

is a Gaussian random vector, and the limit is in the sense of distributions.

Clearly, Theorem 3.2 contains Theorem 3.1. We decided to separately state Theorem 3.1 because its proof is easier. The proof of Theorem 3.2 follows similar logic to Theorem 3.1, so we discuss only the main new points of the former.

Next we remind the reader the definition of a random field (also known as a random function or topological space-valued random variable).

Definition 3.3. [25, p. 182] Let T be a topological space, endowed with its Borel field $\mathcal{B}(T)$. A T -valued random variable X on the probability space $(\Omega, \mathcal{G}, \mathbb{P})$ is a measurable map $X : \Omega \rightarrow T$. In other words, for all $E \in \mathcal{B}(T)$, $\{\omega \in \Omega : X(\omega) \in E\} \in \mathcal{G}$.

Let $D \subset \mathbb{R}^n$ be a bounded domain. Define $C := C(\bar{D}, \mathbb{R})$ to be the collection of all functions continuous up to the boundary $f : \bar{D} \rightarrow \mathbb{R}$ metrized by

$$(3.3) \quad d(f, g) = \max_{\tilde{x} \in \bar{D}} |f(\tilde{x}) - g(\tilde{x})|, \quad f, g \in C.$$

Recall that $G(x)$, $x \in \bar{D}$, is a GRF if $(G(x_1), \dots, G(x_L))$ is a Gaussian random vector for any $L \geq 1$ and any collection of points $x_1, \dots, x_L \in \bar{D}$ [3, Section 1.7]. As is known, a GRF is completely characterized by its mean function $m(x) = \mathbb{E}G(x)$, $x \in D$ and its covariance function $\text{Cov}(x, y) = \mathbb{E}(G(x) - m(x))(G(y) - m(y))$, $x, y \in D$ [3, Section 1.7]. Thus, Theorem 3.2 implies that $N^{\text{rec}}(\tilde{x})$, $\tilde{x} \in \bar{D}$, is a GRF. For simplicity, we drop the dependence of N^{rec} on x_0 from notation.

In the next theorem, we show that $N_{\epsilon}^{\text{rec}}(x_0 + \epsilon \tilde{x}) \rightarrow N^{\text{rec}}(\tilde{x})$, $\tilde{x} \in \bar{D}$, as $\epsilon \rightarrow 0$ weakly, i.e. in distribution as C -valued random variables ([25, p. 185]). Recall that M controls the smoothness of φ (see Assumption 2.6).

Theorem 3.4. *Let D be a bounded domain with a Lipschitz boundary. Suppose the assumptions of Theorem 3.1 hold and $M > n/2$. Then $N_{\epsilon}^{\text{rec}}(x_0 +$*

$\epsilon \check{x}) \rightarrow N^{rec}(\check{x})$, $\check{x} \in \bar{D}$, $\epsilon \rightarrow 0$, as GRFs in the sense of weak convergence. Furthermore, $N^{rec}(\check{x})$, $\check{x} \in \bar{D}$, is a GRF with zero mean and covariance

$$(3.4) \quad \begin{aligned} \text{Cov}(\check{x}, \check{y}) &= C(\check{x} - \check{y}), \\ C(\vartheta) &:= \int_{\mathcal{Y}} (G \star G)(y, \partial_x \Psi(y) \cdot \vartheta) \sigma^2(y, \Psi(y)) dy, \\ (G \star G)(y, \vartheta) &:= \int_{\mathbb{R}^N} G(y, \vartheta + r) G(y, r) dr, \end{aligned}$$

and sample paths of $N^{rec}(\check{x})$ are continuous with probability 1.

4. EXAMPLES

4.1. Classical Radon transform in \mathbb{R}^2 and \mathbb{R}^3 . We begin with the classical RT in \mathbb{R}^2 . The following conventional data parametrization is used:

$$(4.1) \quad y = \alpha, \quad z = p, \quad \Phi(x, \alpha, p) = p - \vec{\alpha} \cdot x, \quad \Psi(x, \alpha) = \vec{\alpha} \cdot x,$$

where $\vec{\alpha} = (\cos \alpha, \sin \alpha)$. Then $\partial_p \Phi(x, \alpha, p) = 1$, so Assumption 2.4(3) is satisfied. From (2.15), $Y_1(x_0, \xi) = \{\alpha \in [0, 2\pi) : \vec{\alpha} \cdot x_0 = 0\}$, which is a set consisting of two points, i.e. it has the upper box-counting dimension of zero, as long as $x_0 \neq 0$. Also, $Y_2(x_0, \check{x}) = \{\alpha \in [0, 2\pi) : \vec{\alpha} \cdot \check{x} = 0\}$ (cf. (2.17)), which is a set of measure zero. Thus, Assumptions 2.8(1,3) are satisfied.

Next consider the classical RT in \mathbb{R}^3 . In this case we use the conventional parametrization

$$(4.2) \quad \begin{aligned} y &= (\alpha, \theta), \quad p = z, \quad \Phi(x, \alpha, \theta, p) = p - \vec{\Theta} \cdot x, \quad \Psi(x, \alpha, \theta) = \vec{\Theta} \cdot x, \\ \vec{\Theta} &:= (\cos \alpha \cos \theta, \cos \alpha \sin \theta, \sin \alpha), \quad \theta \in [0, 2\pi), |\alpha| < \pi/2. \end{aligned}$$

Then $\partial_p \Phi(x, \alpha, \theta, p) = 1$, so Assumption 2.4(3) is satisfied. By (2.15), we compute the Hessian:

$$(4.3) \quad \begin{aligned} \partial_{(\alpha, \theta)}^2 \Psi &= - \begin{pmatrix} (\vec{\theta} \cdot \hat{x}) \cos \alpha + x_3 \sin \alpha & (\vec{\theta}^\perp \cdot \hat{x}) \sin \alpha \\ (\vec{\theta}^\perp \cdot \hat{x}) \sin \alpha & (\vec{\theta} \cdot \hat{x}) \cos \alpha \end{pmatrix}, \\ \vec{\theta} &= (\cos \theta, \sin \theta), \quad \vec{\theta}^\perp = (-\sin \theta, \cos \theta), \quad \hat{x} = (x_1, x_2), \quad x = (\hat{x}, x_3). \end{aligned}$$

Here we have assumed without loss of generality that $\xi = 1$. Clearly, $\det(\partial_{(\alpha, \theta)}^2 \Psi) \equiv 0$ if $\hat{x} = 0$. Thus, all points $x = (0, 0, x_3)$, $x_3 \in \mathbb{R}$, are exceptional, because they violate Assumption 2.8(1). Suppose now $\hat{x} \neq 0$. After simple transformations we obtain

$$(4.4) \quad 2\det(\partial_{(\alpha, \theta)}^2 \Psi) = |\hat{x}|^2 \cos(2\alpha) + x_3(\vec{\theta} \cdot \hat{x}) \sin(2\alpha) + [2(\vec{\theta} \cdot \hat{x})^2 - |\hat{x}|^2].$$

For each $\theta \in [0, 2\pi)$, we can find at most finitely many solutions $|\alpha| < \pi/2$ to $\det(\partial_{(\alpha, \theta)}^2 \Psi) = 0$ and, generically, they depend smoothly on θ . Hence, the sets $Y_1(x, \xi)$, $\xi \neq 0$, have the upper box-counting dimension of one, as long as $\hat{x} \neq 0$. For the cone beam transform, $n = 3$ and $N = 1$, so Assumption 2.8(1) is satisfied.

Finally, $Y_2(x, \check{x}) = \{\vec{\Theta} \in \mathcal{S}^2 : \vec{\Theta} \cdot \check{x} = 0\}$ (cf. (2.17)), which is a set of measure zero in the unit sphere. Thus, Assumption 2.8(3) is satisfied as well.

4.2. **Cone beam transform in \mathbb{R}^3 .** Our next example is the cone beam transform in \mathbb{R}^3 with a circular source trajectory. The detector coordinates are $(u, v) \in \mathbb{R}^2$ (the analog of z), the source coordinate is $s \in [0, 2\pi)$ (the analog of y), see Figure 1, and $n = 3$, $N = 2$. The source trajectory is given by

$$(4.5) \quad P(s) = (R \cos s, R \sin s, 0), \quad 0 \leq s < 2\pi.$$

The (virtual) detector is flat, passes through the origin, and rotates together with the source. Points on the detector are parametrized as follows:

$$(4.6) \quad Z(s, u, v) = u(-\sin s, \cos s, 0) + v(0, 0, 1).$$

For a point $x = (x_1, x_2, x_3) \in \mathbb{R}^3$, its stereographic projection from the source $P(s)$ to a point $(u, v) = (U(x, s), V(x, s))$ in the detector plane is given by

$$(4.7) \quad \begin{aligned} U(x, s) &= T(x, s)(-x_1 \sin s + x_2 \cos s), \quad V(x, s) = T(x, s)x_3, \\ T(x, s) &= [1 - (x_1 \cos s + x_2 \sin s)/R]^{-1}. \end{aligned}$$

The support of f and reconstruction domain \mathcal{X} are contained inside the cylinder $x_1^2 + x_2^2 \leq c < R$. The two key functions are given by

$$(4.8) \quad \Phi(x, s, u, v) = (u - U(x, s), v - V(x, s)), \quad \Psi(x, s) = (U(x, s), V(x, s)).$$

Clearly, $\partial_{(u,v)}\Phi$ is a 2×2 identity matrix, so Assumption 2.4(3) is satisfied.

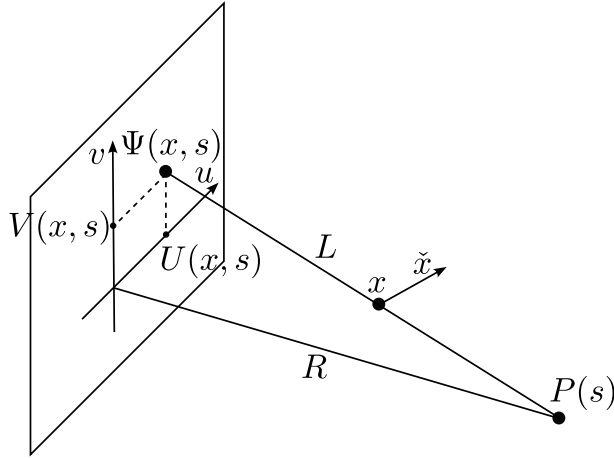


FIGURE 1. Illustration of cone beam geometry.

From (2.15), $Y_1(x, \xi) = \{s \in [0, 2\pi) : \partial_s^2(\xi \cdot \Psi(x, s)) = 0\}$, $\xi \in \mathbb{R}^2 \setminus 0$. Hence, generally, Assumption 2.8(1) is violated if the projection of x onto the detector contains a straight line segment, see Figure 2, left panel. For the circular source trajectory (4.5), this is the case when $x_3 = 0$, i.e. when x is in the plane of the source trajectory, see Figure 2, right panel. As is easy to see, the projection of x to the detector is an ellipse as long as $x_3 \neq 0$. Indeed, from (4.7) we find

$$(4.9) \quad \begin{aligned} (x_2/x_3) \cos s - (x_1/x_3) \sin s &= U/V, \\ (x_1/R) \cos s + (x_2/R) \sin s &= 1 - (x_3/V). \end{aligned}$$

Eliminating $\sin s$ and $\cos s$ gives

$$(4.10) \quad (x_1^2 + x_2^2)V^2 = x_3^2U^2 + R^2(V - x_3)^2.$$

This is an ellipse, because the reconstruction domain is inside the source trajectory, i.e. $x_1^2 + x_2^2 < R^2$. Therefore Assumption 2.8(1) is satisfied if $x_3 \neq 0$.

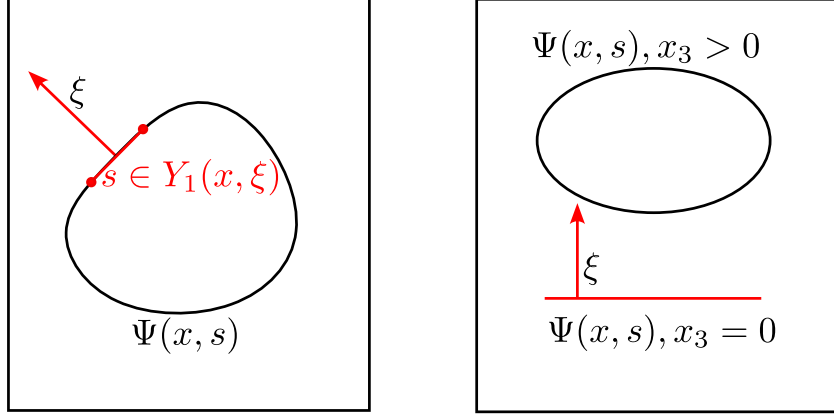


FIGURE 2. Illustration of the case when the set $Y_1(x, \tilde{x})$ is an interval for a general source trajectory (left panel). The right panel illustrates the case of a circular source trajectory.

The meaning of Assumption 2.8(3) is best understood using Figures 1 and 3. We have $Y_2(x, \tilde{x}) = \{s \in [0, 2\pi) : \partial_t \Psi(x + t\tilde{x}, s)|_{t=0} = 0\}$, where $\Psi(x, s)$ is the projection of x to the detector. It is clear from the figures that the directional derivative is zero only when \tilde{x} is along the line $L(x, s)$ through x and the source $P(s)$. This implies that Assumption 2.8(3) is violated only if there exists a line L through x such that the intersection of L with the source trajectory contains a line segment as illustrated in Figure 3. Clearly, for a circular trajectory this does not happen.

5. PROOF OF THEOREM 3.1: CONTRIBUTION OF THE PRINCIPAL SYMBOL

Throughout the proof we make the additional assumption

$$(5.1) \quad a(x, (y, z), \xi) = a_0(x, (y, z), \xi) \equiv 0, \quad (x, (y, z)) \notin \Lambda.$$

This assumption does not affect the validity of Theorem 3.1. One can always modify \mathcal{A} by a smoothing operator so that this condition holds [42, Theorem 2.2, Ch. VI]. See also the last paragraph in section 6.

In view of (2.11), (2.12), consider the integral

$$(5.2) \quad F_\epsilon(u, z') := (2\pi)^{-N} \int_{\mathbb{R}^N} \int_{\mathcal{Z}} a_0(u, z, \xi) \varphi\left(\frac{z - z'}{\epsilon}\right) e^{i\xi \cdot \Phi(u, z)} dz d\xi.$$

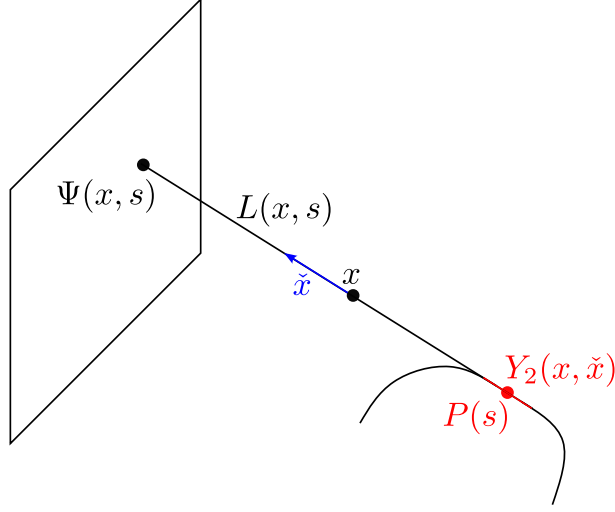


FIGURE 3. Illustration of the case when the set $Y_2(x, \check{x})$ has positive measure. The values $s \in Y_2(x, \check{x})$ parametrize a line segment (shown in red), which is a subset of the source trajectory. The vector \check{x} (shown in blue) is parallel to the line segment. The lines $L(x, s)$, $s \in Y_2(x, \check{x})$, are all the same and contain the segment.

5.1. **An upper bound for $|F_\epsilon(u, z')|$.** Change variable $z \rightarrow w = \Phi(u, z)$ and then $w \rightarrow \check{w} = w/\epsilon$, $\xi \rightarrow \hat{\xi} = \epsilon\xi$:

(5.3)

$$\begin{aligned} F_\epsilon(u, z') &= (2\pi)^{-N} \int_{\mathbb{R}^N} \int_{|\check{w}| \leq \delta/\epsilon} \frac{a_0(u, z, \xi)}{|\det(\partial_z \Phi(u, z))|} \varphi\left(\frac{z - z'}{\epsilon}\right) \epsilon^N e^{i\epsilon\xi \cdot \check{w}} d\check{w} d\xi \\ &= \epsilon^{-\gamma} (2\pi)^{-N} \int_{\mathbb{R}^N} \int_{W_\epsilon(u, z')} a_1(u, z, \hat{\xi}) \varphi\left(\frac{z - z'}{\epsilon}\right) e^{i\hat{\xi} \cdot \check{w}} d\check{w} d\hat{\xi}, \end{aligned}$$

$$a_1(u, z, \xi) := a_0(u, z, \xi) |\det(\partial_z \Phi(u, z))|^{-1}, \quad z = z(\epsilon\check{w}, \epsilon).$$

By (2.8), a_1 is well-defined. Clearly, the matrices $\partial_z \Phi(u, z)$, where $z = z(w, u)$, and $\partial_w z(w, u)$ are the inverses of each other. Here and throughout this section we set

(5.4)

$$\check{v} := (z' - \Psi(u))/\epsilon, \quad W_\epsilon(u, z') := \{\check{w} \in \mathbb{R}^N : (z(\epsilon\check{w}, u) - z')/\epsilon \in \text{supp}(\varphi)\}.$$

Since φ is compactly supported, (2.8) and Assumption 2.4(2) imply:

$$(5.5) \quad \begin{aligned} \text{diam}(W_\epsilon(u, z')) &\leq c, \quad (u, z') \in \Lambda, \quad 0 < \epsilon \ll 1; \\ \check{w} \in W_\epsilon(u, z'), \quad (u, z') \in \Lambda &\text{ implies } [Q^{-1}(u) + O(\epsilon|\check{w}|)] \check{w} \in B(\check{v}, c). \end{aligned}$$

Here $B(\check{v}, c)$ is a ball with center \check{v} and radius c .

Case 1: $|\check{v}| \leq c$. Since φ is compactly supported, (2.8) implies that the domain of integration with respect to \check{w} in (5.3), i.e. the set $W_\epsilon(u, z')$, is a

subset of a disk $|\check{w}| \leq c$. Therefore,

$$(5.6) \quad \begin{aligned} \epsilon^\gamma F_\epsilon(u, z') &= (2\pi)^{-N} \int_{\mathbb{R}^N} H_\epsilon(u, z', \hat{\xi}) d\hat{\xi}, \quad (u, z') \in \Lambda, \\ H_\epsilon(u, z', \hat{\xi}) &:= \int_{|\check{w}| \leq c} a_1(u, z(\epsilon\check{w}, u), \hat{\xi}) \varphi\left(\frac{z(\epsilon\check{w}, u) - z'}{\epsilon}\right) e^{i\hat{\xi} \cdot \check{w}} d\check{w}. \end{aligned}$$

Let M_1 be the smallest integer that satisfies $M_1 > N + \gamma$. Repeated integration by parts with respect to \check{w} gives

$$(5.7) \quad \begin{aligned} H_\epsilon(u, z', \hat{\xi}) &= \int_{|\check{w}| \leq c} (L^T)^{M_1} \left[a_1(u, z, \hat{\xi}) \varphi\left(\frac{z - z'}{\epsilon}\right) \right] e^{i\hat{\xi} \cdot \check{w}} d\check{w}, \\ L &:= (1 + |\hat{\xi}|^2)^{-1} (1 - i\hat{\xi} \cdot \partial_{\check{w}}), \quad z = z(\epsilon\check{w}, u), \quad (u, z') \in \Lambda. \end{aligned}$$

In this integration by parts we use Assumption 2.3(2) and Assumption 2.6. This implies

$$(5.8) \quad |H_\epsilon(u, z', \hat{\xi})| \leq c(1 + |\hat{\xi}|)^{\gamma - M_1}, \quad \hat{\xi} \in \mathbb{R}^N, \quad (u, z') \in \Lambda.$$

The integral on the first line in (5.6) is absolutely convergent because $M_1 > N + \gamma$, hence

$$(5.9) \quad \epsilon^\gamma |F_\epsilon(u, z')| \leq c, \quad \text{if } |\check{v}| \leq c, \quad (u, z') \in \Lambda.$$

Case 2: $|\check{v}| \geq c$. Let $A_1 \in \mathcal{S}'(\mathbb{R}^N)$ be the distribution

$$(5.10) \quad A_1(u, z, \vartheta) := (2\pi)^{-N} \int a_1(u, z, \hat{\xi}) e^{i\hat{\xi} \cdot \vartheta} d\hat{\xi}, \quad (u, z) \in \Lambda, \quad \vartheta \in \mathbb{R}^N.$$

We view ϑ as the argument of A_1 , and u and z – as parameters. As is known, Assumption 2.3(2) implies $A_1 \in C^\infty(\mathbb{R}^N \setminus 0)$ and A_1 is homogeneous of degree $-(N + \gamma)$ [19, Theorems 7.1.16 and 7.1.18]:

$$(5.11) \quad A_1(u, z, t\vartheta) \equiv t^{-(N+\gamma)} A_1(u, z, \vartheta), \quad t > 0.$$

More generally we have $A_1 \in C^\infty(\mathcal{X} \times \mathcal{V} \times (\mathbb{R}^N \setminus 0))$, if u, z, ϑ are all viewed as arguments.

If $|\check{v}|$ is sufficiently large and $\delta > 0$ is sufficiently small (cf. (2.5), (2.7) and (2.8)), the set $W_\epsilon(u, z')$ is bounded away from $\check{w} = 0$. More precisely, $W_\epsilon(u, z') \subset \{\check{w} \in \mathbb{R}^N : |\check{w}| \geq c|\check{v}|\}$ for some $c > 0$ independent of $0 < \epsilon \ll 1$ and $(u, z') \in \Lambda$. Combining with (5.5) this gives

$$(5.12) \quad \epsilon^\gamma F_\epsilon(u, z') = \int_{W_\epsilon(u, z')} A_1(u, z', \check{w}) \varphi\left(\frac{z(\epsilon\check{w}, u) - z'}{\epsilon}\right) d\check{w}, \quad (u, z') \in \Lambda,$$

and (5.11) implies

$$(5.13) \quad \epsilon^\gamma |F_\epsilon(u, z')| \leq c(1 + |\check{v}|)^{-(N+\gamma)} \quad \text{if } |\check{v}| \geq c, \quad (u, z') \in \Lambda.$$

Combining (5.9) and (5.13) gives

$$(5.14) \quad \epsilon^\gamma |F_\epsilon(u, z')| \leq c(1 + |\check{v}|)^{-(N+\gamma)}, \quad (u, z') \in \Lambda.$$

5.2. Approximation of F_ϵ by simpler functions. Replace $z = z(\epsilon\check{w}, u)$ with $z = \Psi(u)$ in the argument of a_1 in (5.3) and define

$$(5.15) \quad F_\epsilon^{(1)}(u, z') := \epsilon^{-\gamma} (2\pi)^{-N} \iint a_1(u, \Psi(u), \hat{\xi}) \varphi\left(\frac{z(\epsilon\check{w}, u) - z'}{\epsilon}\right) e^{i\hat{\xi} \cdot \check{w}} d\check{w} d\hat{\xi}.$$

Since φ is compactly supported,

$$(5.16) \quad |z(\epsilon\check{w}, u) - \Psi(u)| \leq |z(\epsilon\check{w}, u) - z'| + |z' - \Psi(u)| \leq c\epsilon + \epsilon|\check{v}|,$$

cf. (5.4) and (5.5). The following inequality is proven in section A.1.

$$(5.17) \quad \epsilon^\gamma |F_\epsilon(u, z') - F_\epsilon^{(1)}(u, z')| \leq c\epsilon(1 + |\check{v}|)^{-(N+\gamma-1)}, \quad (u, z') \in \Lambda.$$

Next we replace $z(\epsilon\check{w}, u)$ in the arguments of φ in (5.15) and define

$$(5.18) \quad \begin{aligned} \bar{F}_\epsilon(u, z') &:= \epsilon^{-\gamma} (2\pi)^{-N} \iint a_1(u, \Psi(u), \hat{\xi}) \varphi\left(\frac{\bar{z}(\epsilon\check{w}, u) - z'}{\epsilon}\right) e^{i\hat{\xi} \cdot \check{w}} d\check{w} d\hat{\xi}, \\ \bar{z}(w, u) &:= \Psi(u) + Q^{-1}(u)w. \end{aligned}$$

Since φ and its derivatives are bounded, (2.8) implies

$$(5.19) \quad \begin{aligned} &\left| \partial_{\check{w}}^m \left[\varphi\left(\frac{z(\epsilon\check{w}, u) - z'}{\epsilon}\right) - \varphi\left(\frac{\bar{z}(\epsilon\check{w}, u) - z'}{\epsilon}\right) \right] \right| \\ &\leq c[\min(1, \epsilon|\check{w}|^2) + \epsilon|\check{w}|], \quad |m| \leq M_1. \end{aligned}$$

This is where we use that φ has extra smoothness $\varphi \in C_0^{M_1+1}$ (compared with the requirement $\varphi \in C_0^{M_1}$, which suffices for (5.7) to hold). The following claim is proven in section A.2.

$$(5.20) \quad \begin{aligned} \epsilon^\gamma |F_\epsilon^{(1)}(u, z') - \bar{F}_\epsilon(u, z')| &\leq c[\min(1, \epsilon|\check{v}|^2) + \epsilon|\check{v}|] (1 + |\check{v}|)^{-(N+\gamma)}, \\ &(u, z') \in \Lambda. \end{aligned}$$

Combining (5.17) and (5.20) yields

$$(5.21) \quad \epsilon^\gamma |F_\epsilon(u, z') - \bar{F}_\epsilon(u, z')| \leq c \frac{\epsilon(1 + |\check{v}|) + \min(1, \epsilon|\check{v}|^2)}{(1 + |\check{v}|)^{N+\gamma}}, \quad (u, z') \in \Lambda.$$

After simple transformations

$$(5.22) \quad \begin{aligned} \epsilon^\gamma \bar{F}_\epsilon(u, z') &= G(u, \vartheta), \quad G(u, \vartheta) := (2\pi)^{-N} \int_{\mathbb{R}^N} a_2(u, \hat{\mu}) \tilde{\varphi}(\hat{\mu}) e^{i\hat{\mu} \cdot \vartheta} d\hat{\mu}, \\ a_2(u, \hat{\mu}) &:= a_1(u, \Psi(u), Q^{-T}(u)\hat{\mu}), \end{aligned}$$

where $\tilde{\varphi}$ is the Fourier transform of φ . As is easily seen, a_2 satisfies (2.4) with the variable z and set \mathcal{Z} omitted. Recall that $\mathcal{V} = \mathcal{Y} \times \mathcal{Z}$. The main property of the symbol a_2 is that it is independent of z' . Similarly to (5.14),

$$(5.23) \quad |G(u, \vartheta)| \leq c(1 + |\vartheta|)^{-(N+\gamma)}, \quad u \in \mathcal{X} \times \mathcal{Y}, \vartheta \in \mathbb{R}^N.$$

Arguing similarly to (5.6) – (5.14), the assumption $\varphi \in C_0^{M_1+1}(\mathbb{R}^n)$ implies that $G \in C^1(\mathcal{X} \times \mathcal{Y} \times \mathbb{R}^N)$ and

$$(5.24) \quad \begin{aligned} |\partial_u G(u, \vartheta)| &\leq c(1 + |\vartheta|)^{-(N+\gamma)}, \quad |\partial_\vartheta G(u, \vartheta)| \leq c(1 + |\vartheta|)^{-(N+\gamma+1)}, \\ &u \in \mathcal{X} \times \mathcal{Y}, \vartheta \in \mathbb{R}^N. \end{aligned}$$

The second inequality follows because the amplitudes

$$\hat{\mu}_l a_2(u, \hat{\mu}), \quad 1 \leq l \leq N,$$

are homogeneous in $\hat{\mu}$ of degree $\gamma + 1$.

6. PROOF OF THEOREM 3.1: CONTRIBUTION OF THE LOWER ORDER TERMS OF THE FIO \mathcal{A}

Using (5.3) denote

$$(6.1) \quad \Delta a_1(u, z, \xi) := (a(u, z, \xi) - a_0(u, z, \xi)) |\partial_z \Phi(u, z)|^{-1},$$

and

$$(6.2) \quad \begin{aligned} \epsilon^\gamma \Delta F_\epsilon(u, z') &:= (2\pi)^{-N} \int_{\mathbb{R}^N} \Delta H_\epsilon(u, z', \hat{\xi}) d\hat{\xi}, \\ \Delta H_\epsilon(u, z', \hat{\xi}) &:= \int_{W_\epsilon(u, z')} \epsilon^\gamma \Delta a_1(u, z(\epsilon\check{w}, u), \hat{\xi}/\epsilon) \\ &\quad \times \varphi\left(\frac{z(\epsilon\check{w}, u) - z'}{\epsilon}\right) e^{i\hat{\xi} \cdot \check{w}} d\check{w}. \end{aligned}$$

Case 1: $|\check{v}| \leq c$. Using the same operator L as in (5.7), repeated integration by parts with respect to \check{w} gives

$$(6.3) \quad \begin{aligned} \Delta H_\epsilon(u, z', \hat{\xi}) &= \int_{|\check{w}| \leq c} (L^T)^{M_1} \left[\epsilon^\gamma \Delta a_1(u, z, \hat{\xi}/\epsilon) \varphi\left(\frac{z - z'}{\epsilon}\right) \right] e^{i\hat{\xi} \cdot \check{w}} d\check{w}, \\ z &= z(\epsilon\check{w}, u), \end{aligned}$$

This, Assumption 2.3(3), and Assumption 2.6 imply

$$(6.4) \quad \begin{aligned} |\Delta H_\epsilon(u, z', \hat{\xi})| &\leq c\epsilon^\gamma (1 + |\hat{\xi}/\epsilon|)^{\gamma'} (1 + |\hat{\xi}|)^{-M_1} \\ &\leq c\epsilon^{\gamma - \gamma'} (1 + |\hat{\xi}|)^{\gamma' - M_1}, \quad \hat{\xi} \in \mathbb{R}^N, (u, z') \in \Lambda. \end{aligned}$$

The integral on the first line in (6.2) is absolutely convergent because $M_1 > N + \gamma'$, hence

$$(6.5) \quad \epsilon^\gamma |\Delta F_\epsilon(u, z')| = O(\epsilon^{\gamma - \gamma'}), \quad |\check{v}| \leq c, (u, z') \in \Lambda.$$

Case 2: $|\check{v}| \geq c$. When $w = 0$ is not in the domain of integration, we have

$$(6.6) \quad \begin{aligned} \Delta F_\epsilon(u, z') &= \int_{|w| \leq \delta} \Delta A_1(u, z(w, u), w) \varphi\left(\frac{z(w, u) - z'}{\epsilon}\right) dw, \\ \Delta A_1(u, z, \vartheta) &:= (2\pi)^{-N} \int_{\mathbb{R}^N} \Delta a_1(u, z, \xi) e^{i\xi \cdot \vartheta} d\xi. \end{aligned}$$

Since $\gamma > -N/2$, we can always assume that $N + \gamma' > 0$. By assumption 2.3(3) and [1, Theorem 5.12],

$$(6.7) \quad |\Delta A_1(u, z, \vartheta)| \leq c|\vartheta|^{-(N + \gamma')}, \quad (u, z) \in \Lambda, 0 < |\vartheta| \leq c.$$

The fact that the amplitude $\Delta a_1(u, z, \xi)$ is not smooth at the origin $\xi = 0$ is irrelevant, since this part contributes a bounded term. We have used here that ϑ is confined to a bounded set, and the goal of (6.7) is to provide a bound near $\vartheta = 0$. Substituting (6.7) into the first equation in (6.6) and

changing variable $w = \epsilon \check{w}$ gives using (5.5) and that $W_\epsilon(u, z') \subset \{\check{w} \in \mathbb{R}^N : |\check{w}| \geq c|\check{v}|\}$:

$$(6.8) \quad \epsilon^\gamma |\Delta F_\epsilon(u, z')| \leq c\epsilon^{\gamma-\gamma'} (1 + |\check{v}|)^{-(N+\gamma')}, \quad |\check{v}| \geq c, (u, z') \in \Lambda.$$

Combining with (6.5) yields

$$(6.9) \quad \epsilon^\gamma |\Delta F_\epsilon(u, z')| \leq c\epsilon^{\gamma-\gamma'} (1 + |\check{v}|)^{-(N+\gamma')}, \quad (u, z') \in \Lambda.$$

Recall that, by construction, $\Delta F_\epsilon(u, z') = 0$ if $(u, z') \in (\mathcal{X} \times \mathcal{V}) \setminus \Lambda$.

Suppose now that K is a smoothing operator. Such an operator may be needed to ensure that $a(u, z, \xi) \equiv 0$ if $(u, z) \notin \Lambda$ (see (5.1)). The analog of (5.2) is

$$(6.10) \quad F_\epsilon(u, z') := \int_{\mathcal{Z}} K(u, z) \varphi((z - z')/\epsilon) dz = O(\epsilon^N), \quad \epsilon \rightarrow 0,$$

uniformly in $(u, z') \in \mathcal{X} \times \mathcal{V}$.

7. END OF PROOF OF THEOREM 3.1 AND PROOF OF THEOREM 3.2

In what follows we take $x = x_0 + \epsilon \check{x}$. By (5.24),

$$(7.1) \quad G\left(x, y, \frac{z' - \Psi(x, y)}{\epsilon}\right) = G\left(x_0, y, \frac{z' - \Psi(x_0, y)}{\epsilon} - \partial_x \Psi(x_0, y) \cdot \check{x}\right) + \frac{O(\epsilon)}{(1 + |\check{v}|)^{N+\gamma}}.$$

In this section x_0 is fixed and dropped from most notation. Since $z' = z_k = \epsilon k$ (cf. (2.9), (2.11), (2.12), and (5.2)), reconstruction from noise can be written as follows

$$(7.2) \quad N_\epsilon^{\text{rec}}(x_0 + \epsilon \check{x}) = \kappa_\epsilon \sum_{(y_j, z_k) \in \mathcal{V}} [G(y_j, k - b_j) + R_{j,k}] \eta_{j,k},$$

$$b_j := \partial_x \Psi(x_0, y_j) \cdot \check{x} + (\Psi(x_0, y_j)/\epsilon), \quad \kappa_\epsilon := \epsilon^{-\gamma} \epsilon_y^{n-N},$$

where $R_{j,k}$ is the remainder. By (5.21), (6.9), (6.10), and (7.1) the remainder satisfies

$$(7.3) \quad |R_{j,k}| \leq c \frac{\epsilon(1+t) + \min(1, \epsilon t^2)}{(1+t)^{N+\gamma}} + c \frac{\epsilon^{\gamma-\gamma'}}{(1+t)^{N+\gamma'}} + O(\epsilon^{N+\gamma}),$$

$$t = |k - b_j|, \quad (y_j, z_k) \in \mathcal{V}.$$

The following result is proven in appendix B. Its proof requires Assumption 2.8(1).

Lemma 7.1. *Suppose the assumptions of Theorem 3.1 are satisfied. For any $\xi \in \mathbb{R}^N \setminus 0$, $u \in \mathbb{Z}^{n-N}$, and any $\delta > 0$ sufficiently small, there exist $p > 0$ and a finite collection of hypercubes $\mathcal{B}_k \subset \mathbb{R}^{n-N}$ such that*

$$(7.4) \quad \{y \in \mathcal{Y} : |\partial_y(\xi \cdot \Psi(x_0, y)) - u| \leq p\} \subset \cup_k \mathcal{B}_k, \quad \sum_k \text{Vol}(\mathcal{B}_k) \leq \delta.$$

We have the following lemma, which is proven in appendix C. The proof uses Lemma 7.1.

Lemma 7.2. *Suppose the assumptions of Theorem 3.1 are satisfied. With b_j and κ_ϵ defined in (7.2), one has*

$$(7.5) \quad \lim_{\epsilon \rightarrow 0} \frac{\kappa_\epsilon^3 \sum_{(y_j, z_k) \in \mathcal{V}} |G(y_j, k - b_j) + R_{j,k}|^3 \mathbb{E}|\eta_{j,k}|^3}{[\kappa_\epsilon^2 \sum_{(y_j, z_k) \in \mathcal{V}} (G(y_j, k - b_j) + R_{j,k})^2 \mathbb{E}\eta_{j,k}^2]^{3/2}} = 0.$$

Lemma 7.2 implies that the family of random variables $N_\epsilon^{\text{rec}}(x_0 + \epsilon \tilde{x})$, $\epsilon > 0$, satisfies the Lyapunov condition for triangular arrays [4, Definition 11.1.3]. By [4, Corollary 11.1.4], $N^{\text{rec}} := \lim_{\epsilon \rightarrow 0} N_\epsilon^{\text{rec}}(x_0 + \epsilon \tilde{x})$ is a Gaussian random variable, where the limit is in the sense of convergence in distribution. This completes the proof of Theorem 3.1.

7.1. Finite-dimensional distributions. Proof of Theorem 3.2. Recall that the random vector $\vec{N}_\epsilon^{\text{rec}}$ is defined in the paragraph preceding Theorem 3.2. Pick any vector $\vec{\theta} \in \mathbb{R}^L$. By (7.2)

$$(7.6) \quad \zeta_\epsilon := \vec{\theta} \cdot \vec{N}_\epsilon^{\text{rec}} = \kappa_\epsilon \sum_{(y_j, z_k) \in \mathcal{V}} \left[\sum_{l=1}^L \theta_l (G(y_j, k - b_j^{(l)}) + R_{j,k}^{(l)}) \right] \eta_{j,k},$$

$$b_j^{(l)} := \partial_x \Psi(x_0, y_j) \cdot \tilde{x}_l + (\Psi(x_0, y_j)/\epsilon).$$

To show that $\vec{N}_\epsilon^{\text{rec}}$ converges in distribution to a Gaussian random vector, it suffices to show that for any $\vec{\theta} \in \mathbb{R}^L \setminus 0$, $\lim_{\epsilon \rightarrow 0} \zeta_\epsilon$ is a Gaussian random variable [4, Theorem 10.4.5]. The following result is proven in appendix E.

Lemma 7.3. *Suppose the assumptions of Theorem 3.2 are satisfied. With $b_j^{(l)}$ defined in (7.6) and κ_ϵ defined in (7.2), one has*

$$(7.7) \quad \lim_{\epsilon \rightarrow 0} \frac{\kappa_\epsilon^3 \sum_{(y_j, z_k) \in \mathcal{V}} |\sum_{l=1}^L \theta_l (G(y_j, k - b_j^{(l)}) + R_{j,k}^{(l)})|^3 \mathbb{E}|\eta_{j,k}|^3}{[\kappa_\epsilon^2 \sum_{(y_j, z_k) \in \mathcal{V}} [\sum_{l=1}^L \theta_l (G(y_j, k - b_j^{(l)}) + R_{j,k}^{(l)})]^2 \mathbb{E}\eta_{j,k}^2]^{3/2}} = 0.$$

It follows from [4, Corollary 11.1.4] that $\zeta = \lim_{\epsilon \rightarrow 0} \zeta_\epsilon$ is a Gaussian random variable. Hence, by [4, Theorem 10.4.5], $\lim_{\epsilon \rightarrow 0} \vec{N}_\epsilon^{\text{rec}}$ is a Gaussian random vector, where as before, the limit is in the sense of convergence in distribution. This completes the proof of Theorem 3.2.

8. PROOF OF THEOREM 3.4

We use the following definition and theorem.

Definition 8.1 ([25, p. 189]). Let \mathbb{P}_n be the distribution of a C -valued random variable X_n , $1 \leq n \leq \infty$. The collection (\mathbb{P}_n) is tight if for all $\delta \in (0, 1)$, there exists a compact set $\Gamma_\delta \in C$ such that $\sup_n \mathbb{P}(X_n \notin \Gamma_\delta) \leq \delta$.

Theorem 8.2 ([25, Proposition 3.3.1]). *Suppose X_n , $1 \leq n \leq \infty$, are C -valued random variables. Then $X_n \rightarrow X_\infty$ weakly (i.e., the distribution of X_n converges to that of X_∞ , see [25, p. 185]) provided that:*

- (1) *Finite dimensional distributions of X_n converge to that of X_∞ .*
- (2) *(X_n) is a tight sequence.*

Theorem 3.2 asserts that all finite-dimension distributions of $N_\epsilon^{\text{rec}}(x_0 + \epsilon\tilde{x})$ converge to that of the GRF $N^{\text{rec}}(\tilde{x})$. Thus it remains to verify property (2) of Theorem 8.2. To this end, we introduce the sets

$$(8.1) \quad \Gamma_\delta := \{f \in C : \|f\|_{W^{M,2}(D)}^2 \leq 1/\delta\}.$$

Recall that M controls the smoothness of φ (see Assumption 2.6). Recall also that $W^{l,p}(D)$ is the closure of $C^\infty(\bar{D})$ in the norm:

$$(8.2) \quad \|f\|_{l,p} := \left(\int_D \sum_{|m| \leq l} |\partial_x^m f(x)|^p dx \right)^{1/p}, \quad f \in C^\infty(\bar{D}).$$

Since D has a Lipschitz continuous boundary and $M > n/2$, from [16, Theorem 7.26, p. 171] it follows that the imbedding $W^{M,2}(D) \hookrightarrow C(\bar{D})$ is compact. Hence the set $\Gamma_\delta \subset C$ is compact for every $\delta > 0$.

Adopting the argument (5.4)–(5.14) to the full symbol of \mathcal{A} (which only requires replacing (5.11) with [1, Theorem 5.12]), it is easy to see that

$$(8.3) \quad \begin{aligned} \epsilon^\gamma |\partial_{\tilde{x}}^m F_\epsilon(x, y, z)| &\leq c(1 + |z - \Psi(x, y)|/\epsilon)^{-(N+\gamma)}, \\ x = x_0 + \epsilon\tilde{x}, \tilde{x} \in D, (y, z) \in \mathcal{V}, m \in \mathbb{N}_0^n, |m| \leq M. \end{aligned}$$

This calculation uses Assumption 2.3 and that the derivatives $\varphi^{(m)}(w)$, $|m| \leq M$, where $M > n/2$, are bounded. Therefore

$$(8.4) \quad \begin{aligned} &\mathbb{E}(\partial_{\tilde{x}}^m N_\epsilon^{\text{rec}}(x_0 + \epsilon\tilde{x}))^2 \\ &= \epsilon^{n-N} \sum_{(y_j, z_k) \in \mathcal{V}} [\epsilon^\gamma \partial_{\tilde{x}}^m F_\epsilon(x, y_j, z_k)]^2 \sigma^2(y_j, z_k) \\ &\leq c\epsilon^{n-N} \sum_{(y_j, z_k) \in \mathcal{V}} [1 + |k - (\Psi(x_0, y_j)/\epsilon)|]^{-2(N+\gamma)} \leq c, \quad \tilde{x} \in D. \end{aligned}$$

This implies that $\mathbb{E}\|N_\epsilon^{\text{rec}}(x_0 + \epsilon\tilde{x})\|_{W^{M,2}(D)}^2 \leq c$ for all $\epsilon > 0$. By the Chebyshev inequality,

$$(8.5) \quad \mathbb{P}(N_\epsilon^{\text{rec}}(x_0 + \epsilon\tilde{x}) \notin \Gamma_\delta) = \mathbb{P}(\|N_\epsilon^{\text{rec}}(x_0 + \epsilon\tilde{x})\|_{W^{M,2}(D)}^2 \geq 1/\delta) \leq c\delta.$$

Therefore $(N_\epsilon^{\text{rec}}(x_0 + \epsilon\tilde{x}))$, $0 < \epsilon \ll 1$, is a tight sequence.

By Theorem 8.2, $N_\epsilon^{\text{rec}}(x_0 + \epsilon\tilde{x}) \rightarrow N^{\text{rec}}(\tilde{x})$, $\tilde{x} \in \bar{D}$, in distribution as C -valued random variables. Since C is a complete metric space, it follows that $N^{\text{rec}} \in C$ has continuous sample paths with probability 1.

By the linearity of the expectation, $N^{\text{rec}}(\tilde{x})$ is a zero mean GRF. To completely characterize this GRF, we calculate its covariance $\text{Cov}(\tilde{x}, \tilde{y}) = \lim_{\epsilon \rightarrow 0} \mathbb{E}(N_\epsilon^{\text{rec}}(\tilde{x})N_\epsilon^{\text{rec}}(\tilde{y}))$, $\tilde{x}, \tilde{y} \in D$. In fact, essentially this has already been done in the proof of Lemma 7.3: equation (E.3) implies (3.4).

9. NUMERICAL EXPERIMENTS

For a numerical experiment we consider cone beam local tomography reconstruction, see subsection 4.2 and Figure 1. Recall that the detector coordinates are $(u, v) \in \mathbb{R}^2$ and the source coordinate is $s \in [0, 2\pi)$, see (4.5), (4.6). The data are given at the points:

$$(9.1) \quad s = \Delta sj, \quad u = \epsilon k_1, \quad v = \epsilon k_2, \quad j, k_1, k_2 \in \mathbb{Z}.$$

To reconstruct an image we backproject the second derivative of the cone beam transform along detector rows (i.e., along u). In the continuous case the reconstruction formula is as follows.

$$(9.2) \quad \begin{aligned} f_\epsilon^{\text{rec}}(x) &= \int_0^{2\pi} \partial_u^2 g(s, U(x, s), V(x, s)) ds \\ &= \int_0^{2\pi} \iint_{\mathbb{R}^2} \delta''(U(x, s) - u) \delta(V(x, s) - v) g(s, u, v) du dv ds. \end{aligned}$$

This is local tomography reconstruction [31, 35]. Representing the two delta-functions in terms of their Fourier transforms, we see that the complete symbol of the operator \mathcal{A} coincides with its principal symbol and $\gamma = 2$. Reconstruction from discrete data (consisting only of noise) is given by

$$(9.3) \quad N_\epsilon^{\text{rec}}(x) = \frac{\Delta s}{\epsilon^2} \sum_{j,k} \varphi''\left(\frac{U(x, s) - \epsilon k_1}{\epsilon}\right) \varphi\left(\frac{V(x, s) - \epsilon k_2}{\epsilon}\right) \eta_{j,k}.$$

By (5.2),

$$(9.4) \quad \begin{aligned} F_\epsilon(x, s, u', v') &= \int_{\mathbb{R}^2} \delta''(U(x, s) - u) \delta(V(x, s) - v) \\ &\quad \times \varphi((u - u')/\epsilon) \varphi((v - v')/\epsilon) du dv \\ &= \frac{1}{\epsilon^2} \varphi''\left(\frac{U(x, s) - u'}{\epsilon}\right) \varphi\left(\frac{V(x, s) - v'}{\epsilon}\right). \end{aligned}$$

The function Φ is linear in (u, v) (cf. (4.8)) and the symbol of \mathcal{A} is independent of (u, v) , hence $\bar{F}_\epsilon \equiv F_\epsilon$. Then, by (5.22), $G(\vartheta) = \varphi''(\vartheta_1) \varphi(\vartheta_2)$. Note that G does not depend on x and s . From (3.4),

$$(9.5) \quad (G \star G)(\vartheta) = \int_{\mathbb{R}} \varphi''(\vartheta_1 + r_1) \varphi''(r_1) dr_1 \int_{\mathbb{R}} \varphi(\vartheta_2 + r_2) \varphi(r_2) dr_2.$$

Finally, the covariance function is given by (cf. (3.4))

$$(9.6) \quad C(\vartheta) = \int_0^{2\pi} (G \star G)(\partial_x(U(x_0, s), V(x_0, s))\vartheta) \sigma^2(s, U(x_0, s), V(x_0, s)) ds,$$

where $\vartheta = \check{x}_1 - \check{x}_2$. The derivatives $\partial_x U(x_0, s)$ and $\partial_x V(x_0, s)$ are computed explicitly using (4.7).

Next we describe a numerical experiment to verify the obtained results, namely Theorem 3.4. The center of a local patch and two nearby points $x_k = x_0 + \epsilon \check{x}_k$, $k = 1, 2$ are selected as follows:

$$(9.7) \quad \begin{aligned} x_0 &= (2.7, -3.1, 0.8), \\ \check{x}_1 &= (2.159, 3.075, -0.418), \quad \check{x}_2 = (2.546, -2.974, 0.983). \end{aligned}$$

The radius of the source trajectory is $R = 10$ (see (4.5)). The values of $\eta_{j,k}$ are computed by the formula:

$$(9.8) \quad \begin{aligned} \eta_{j,k} &= (\epsilon^2 / \Delta s) h(s_j, u_{k_1}, v_{k_2}) \nu_{j,k}, \\ h(s, u, v) &= (1 + 0.5 \sin(2s))(1 - 0.4 \cos u)(1 + 0.6 \sin v), \end{aligned}$$

and $\nu_{j,k}$ are i.i.d. random variables drawn from the uniform distribution on $[-1, 1]$. Comparing with (2.10), we see that $(\epsilon^2 / \Delta s)^2 = \epsilon^{2\gamma} / \Delta s^{n-N}$ (because $\epsilon_y = \Delta s$, $\gamma = 2$ and $n - N = 2$) and $\sigma^2(s, u, v) = (1/3)h^2(s, u, v)$. In the

experiment, $2 \cdot 10^4$ realizations of noisy sinograms, i.e. the sets $\{\eta_{j,k}\}$, have been used. We set

$$(9.9) \quad \Delta s = 2\pi/500, \quad \epsilon = \Delta u = \Delta v = 0.05.$$

The kernel function φ is obtained by convolving the interpolation kernel $(1 - |s|)_+$ and the smoothing kernel $c_l(1 - (s/a)^2)_+^l$:

$$(9.10) \quad \varphi(t) = \frac{(2l+1)!!}{2a(2l)!!} \int_{-1}^1 (1 - |s|) [1 - ((t-s)/a)^2]_+^l ds, \quad a = 2.5, \quad l = 3.$$

Let us summarize the results of the experiment. At x_0 , the sample variance is 0.488 and predicted variance is 0.485. The latter is obtained using (9.6) with $\vartheta = 0$. The observed probability density function (PDF), i.e., the normalized histogram, and predicted PDF are shown in Figure 4. The histogram is computed using 21 bins. The predicted PDF, which is a Gaussian with zero mean and variance 0.485, is computed by evaluating the Gaussian density at the center of each bin. The relative mismatch between the observed and predicted discretized PDFs (denoted P_o and P_p , respectively) is found to be $\|P_o - P_p\|_1 / \|P_p\|_1 = 0.021$. Here and below, $\|\cdot\|_1$ denotes the appropriate discrete l^1 norm (the sum of absolute values of the entries of a vector or matrix).

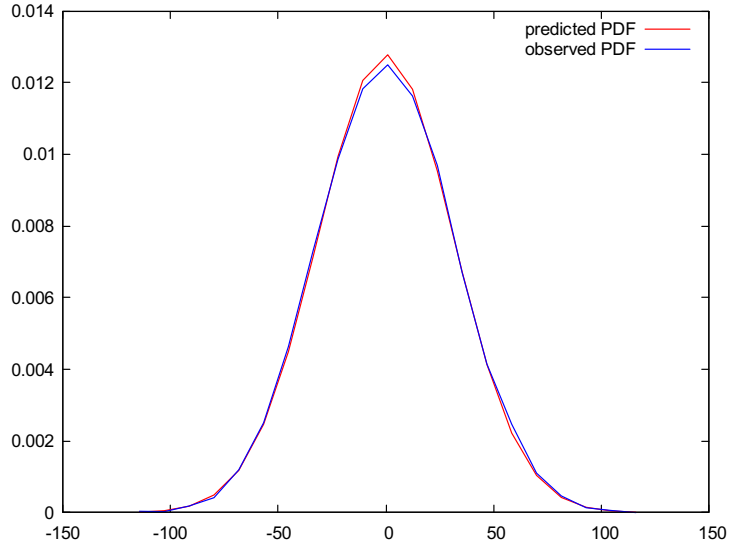


FIGURE 4. Observed PDF and predicted PDF for the random variable $N_\epsilon^{\text{rec}}(\tilde{x} = 0)$ (i.e., at x_0 in the original coordinates). The x -axis represents the values of the random variable.

Next we test the accuracy of our two-point estimates. For the two points \tilde{x}_1 and \tilde{x}_2 in (9.7), the observed and predicted covariances and the relative error between them are found to be

$$(9.11) \quad \text{Cov}_o = \begin{pmatrix} 0.479 & 0.013 \\ 0.013 & 0.458 \end{pmatrix}, \quad \text{Cov}_p = \begin{pmatrix} 0.485 & 0.011 \\ 0.011 & 0.485 \end{pmatrix},$$

$$\|\text{Cov}_o - \text{Cov}_p\|_1 / \|\text{Cov}_p\|_1 = 0.035.$$

The diagonal entries of the covariance matrix Cov_p are equal $C(0)$, and off-diagonal elements are equal $C(\tilde{x}_1 - \tilde{x}_2)$. The observed 2D PDF and predicted 2D PDF are shown in Figure 5. The histogram is computed using 21×21 bins. The predicted PDF is computed by evaluating the predicted Gaussian density at the center of each bin. The relative mismatch between the observed and predicted discretized PDFs is found to be $\|P_o - P_p\|_1 / \|P_p\|_1 = 0.079$, which is quite small as well.

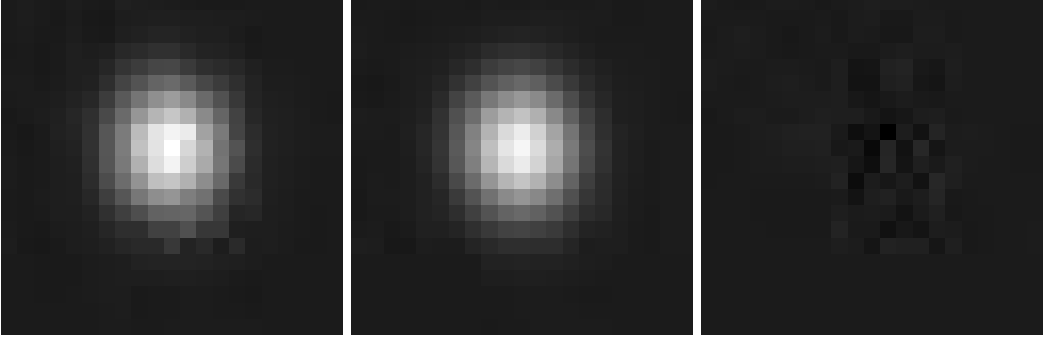


FIGURE 5. Observed PDF (left), predicted PDF (center), and their difference (right) for the random vector $(N_\epsilon^{\text{rec}}(\tilde{x}_1), N_\epsilon^{\text{rec}}(\tilde{x}_2))$. The display range is $[-2\text{E-}5, 1.7\text{E-}4]$ for all three figures. The horizontal and vertical axes represent the values of $N_\epsilon^{\text{rec}}(\tilde{x}_1)$ and $N_\epsilon^{\text{rec}}(\tilde{x}_2)$, respectively.

APPENDIX A. PROOFS OF TWO AUXILIARY RESULTS

A.1. **Proof of (5.17).** By (5.6) and (5.15), we have to estimate the quantity

$$(A.1) \quad J := (2\pi)^{-N} \int_{\mathbb{R}^N} \int_{W_\epsilon(u, z')} \Delta a_1(u, \epsilon \check{w}, \hat{\xi}) \varphi\left(\frac{z(\epsilon \check{w}, u) - z'}{\epsilon}\right) e^{i\hat{\xi} \cdot \check{w}} d\check{w} d\hat{\xi},$$

$$\Delta a_1(u, w, \hat{\xi}) := a_1(u, z(w, u), \hat{\xi}) - a_1(u, \Psi(u), \hat{\xi}), \quad (u, z') \in \Lambda.$$

Suppose $|\check{v}| \leq c$. By (5.16) and using Assumption 2.3(2) and Assumption 2.6, the analog of (5.8) becomes

$$(A.2) \quad |H_\epsilon(u, z', \hat{\xi})| \leq c\epsilon(1 + |\hat{\xi}|)^{\gamma - M_1}, \quad \hat{\xi} \in \mathbb{R}^N.$$

Similarly to (5.7), integration by parts to prove (A.2) involves $\partial_{\check{w}}$ rather than ∂_w . Integrating with respect to $\hat{\xi}$ gives $|J| \leq c\epsilon$.

If $|\check{v}| \geq c$, (5.12) implies

$$(A.3) \quad J = \int_{W_\epsilon(u, z')} [A_1(u, z', \check{w}) - A_1(u, \Psi(u), \check{w})] \varphi\left(\frac{z(\epsilon \check{w}, u) - z'}{\epsilon}\right) d\check{w}.$$

By Assumption 2.3(2), the kernel A_1 depends smoothly on z' . Therefore (5.11) yields:

$$(A.4) \quad |J| \leq c\epsilon|\check{v}|(1 + |\check{v}|)^{-(N+\gamma)} \text{ if } |\check{v}| \geq c.$$

The desired assertion (5.17) now follows.

A.2. **Proof of (5.20).** We need to estimate the quantity

$$\begin{aligned}
 J &:= (2\pi)^{-N} \int_{\mathbb{R}^N} \Delta H_\epsilon(u, z', \hat{\xi}) d\hat{\xi}, \quad (u, z') \in \Lambda, \\
 \text{(A.5)} \quad \Delta H_\epsilon(u, z', \hat{\xi}) &:= \int_{\mathbb{R}^N} a_1(u, \Psi(u), \hat{\xi}) \\
 &\quad \times \left[\varphi\left(\frac{z(\epsilon\check{w}, u) - z'}{\epsilon}\right) - \varphi\left(\frac{\bar{z}(\epsilon\check{w}, u) - z'}{\epsilon}\right) \right] e^{i\hat{\xi} \cdot \check{w}} d\check{w}.
 \end{aligned}$$

Using (5.19) and Assumptions 2.3(2) and 2.6, the analogs of (5.7) and (5.8) become

$$\begin{aligned}
 \text{(A.6)} \quad |\Delta H_\epsilon(u, z', \hat{\xi})| &\leq c(1 + |\hat{\xi}|)^{\gamma - M_1} \int_{|\check{w}| \leq c} [\min(1, \epsilon|\check{w}|^2) + \epsilon|\check{w}|] d\check{w} \\
 &\leq c\epsilon(1 + |\hat{\xi}|)^{\gamma - M_1}, \quad \hat{\xi} \in \mathbb{R}^N, |\check{v}| \leq c.
 \end{aligned}$$

Integrating with respect to $\hat{\xi}$ gives $|J| \leq c\epsilon$, $|\check{v}| \leq c$. As before, we need $\varphi \in C_0^{M_1+1}(\mathbb{R}^N)$ for this to work. Suppose now $|\check{v}| \geq c$. Similarly to (A.3),

$$\text{(A.7)} \quad J = \int_{\mathbb{R}^n} A_1(u, \Psi(u), \check{w}) \left[\varphi\left(\frac{z(\epsilon\check{w}, u) - z'}{\epsilon}\right) - \varphi\left(\frac{\bar{z}(\epsilon\check{w}, u) - z'}{\epsilon}\right) \right] d\check{w}.$$

By (5.19), the analog of (5.13) becomes

$$\text{(A.8)} \quad |J| \leq c[\min(1, \epsilon|\check{v}|^2) + \epsilon|\check{v}|](1 + |\check{v}|)^{-(N+\gamma)} \text{ if } |\check{v}| \geq c.$$

Even though the integrals (A.5) and (A.7) involve φ of two different arguments, the domain of integration of each of them has the same key properties as $W_\epsilon(u, z')$: it is a uniformly bounded set, it is confined to a ball $|\check{w}| \leq c$ if $|\check{v}| \leq c$, and it is a subset of $\{\check{w} \in \mathbb{R}^N : |\check{w}| \geq c|\check{v}|\}$ if $|\check{v}| \geq c$.

The desired assertion (5.20) now follows.

APPENDIX B. PROOF OF LEMMA 7.1

Since x_0 is fixed, in this and the remaining appendices we omit x_0 from most notations.

Let $d_0(\xi)$ be the upper box-counting dimension of $Y_1(\xi)$, see Definition 2.7 and (2.15). Then $Y_1(\xi)$ can be covered by no more than $(1/\delta_1)^d$ (hyper)cubes $\mathcal{B}_k \subset \mathbb{R}^{n-N}$ with side length δ_1 for any $d > d_0(\xi)$ and $\delta_1 > 0$ sufficiently small. Replace each \mathcal{B}_k with a (slightly) larger open cube $\mathcal{B}_k^{(1)}$ (say, twice the volume), which has the same center and orientation as \mathcal{B}_k . The sum of their $(n - N)$ -dimensional volumes satisfies

$$\sum_k \text{Vol}(\mathcal{B}_k^{(1)}) \leq c\delta_1^{(n-N)-d} \rightarrow 0, \quad \delta_1 \rightarrow 0,$$

because we can take $d_0(\xi) < d < n - N$. Find $\delta_1 > 0$ so that $\sum_k \text{Vol}(\mathcal{B}_k^{(1)}) \leq \delta/2$. By construction, the interior of $\cup_k \mathcal{B}_k^{(1)}$ is a neighborhood of $Y_1(\xi)$.

Pick any $u \in \mathbb{Z}^{n-N}$ and $\xi \in \mathbb{R}^N \setminus 0$. By construction, $\det(\partial_y^2(\xi \cdot \Psi))$ is bounded away from zero on the set $\mathcal{Y} \setminus (\cup_k \mathcal{B}_k^{(1)})$. Therefore, there are finitely many solutions to the equation $\partial_y(\xi \cdot \Psi(y)) = u$ in $\mathcal{Y} \setminus (\cup_k \mathcal{B}_k^{(1)})$. Cover these solutions by finitely many sufficiently small open cubes $\mathcal{B}_k^{(2)}$, which satisfy $\sum_k \text{Vol}(\mathcal{B}_k^{(2)}) \leq \delta/2$. Let \mathcal{B} denote the union of all the cubes $\mathcal{B}_k^{(1)}, \mathcal{B}_k^{(2)}$. By

construction, the interior of \mathcal{B} is a neighborhood of the set of solutions to $\partial_y(\xi \cdot \Psi(y)) = u$, $y \in \mathcal{Y}$. Therefore,

$$(B.1) \quad \sum_k \text{Vol}(\mathcal{B}_k^{(1)}) + \sum_k \text{Vol}(\mathcal{B}_k^{(2)}) \leq \delta, \quad \inf_{y \in \mathcal{Y} \setminus \mathcal{B}} |\partial_y(\xi \cdot \Psi(y)) - u| =: p > 0,$$

and the lemma is proven.

APPENDIX C. PROOF OF LEMMA 7.2

Let D_ϵ be the expression in brackets in the denominator in (7.5). By (2.10),

$$(C.1) \quad \begin{aligned} & \kappa_\epsilon^2 \sum_{z_k \in \mathcal{Z}} |(G(y_j, k - b_j) + R_{j,k})^2 - G^2(y_j, k - b_j)| \mathbb{E} \eta_{j,k}^2 \\ & \leq c \epsilon^{n-N} \sum_{z_k \in \mathcal{Z}} [R_{j,k}^2 + |G(y_j, k - b_j)| |R_{j,k}|]. \end{aligned}$$

See (7.2) for the definitions of κ_ϵ and b_j . Using (5.23) and (7.3), straightforward calculations shows that

$$(C.2) \quad \sum_{z_k \in \mathcal{Z}} R_{j,k}^2 \leq c \epsilon^\delta, \quad \sum_{z_k \in \mathcal{Z}} |G(y_j, k - b_j)| |R_{j,k}| \leq c \epsilon^\delta$$

for some $\delta > 0$ as long as $\gamma > -N/2$. Therefore, by (2.10)

$$(C.3) \quad D_\epsilon = \epsilon_y^{n-N} \sum_{(y_j, z_k) \in \mathcal{V}} G^2(y_j, k - b_j) \sigma^2(y_j, z_k) + O(\epsilon^\delta).$$

Define

$$(C.4) \quad \psi(y, r) := \sum_{k \in \mathbb{Z}^N} G^2(y, k - r), \quad y \in \mathcal{Y}, r \in \mathbb{R}^N.$$

By (5.23) the series is absolutely convergent. It is easy to see that

$$(C.5) \quad \psi(y, r + m) = \psi(y, r), \quad y \in \mathcal{Y}, r \in \mathbb{R}^N, m \in \mathbb{Z}^N.$$

Replace z_k with $\Psi(y_j)$ in the arguments of σ^2 in (C.3) to obtain

$$(C.6) \quad D_\epsilon = \epsilon_y^{n-N} \sum_{y_j \in \mathcal{Y}} \psi(y_j, b_j) \sigma^2(y_j, \Psi(y_j)) + O(\epsilon^\delta).$$

Indeed, consider the sum with respect to k . By the definition of b_j in (7.2) we have $z_k - \Psi(y_j) = \epsilon(k - b_j + O(1))$. By (5.23) and Lipschitz continuity of σ :

$$(C.7) \quad \begin{aligned} & \sum_{|k| \leq O(1/\epsilon)} G^2(y, k - b_j) |\sigma^2(y, \epsilon k) - \sigma^2(y, \Psi(y_j))| \\ & \leq c \sum_{|k| \leq O(1/\epsilon)} \epsilon(1 + |k - b_j|)(1 + |k - b_j|)^{-2(N+\gamma)} = O(\epsilon^a) \rightarrow 0, \end{aligned}$$

where $a = \min(1, 2\gamma + N)$. The assumption $\gamma > -N/2$ implies $a > 0$. Summing over $y_j \in \mathcal{Y}$ and accounting for the factor ϵ_y^{n-N} proves the claim.

Using arguments similar to [20], we prove in Section D the following result

$$(C.8) \quad \lim_{\epsilon \rightarrow 0} D_\epsilon = \int_{\mathcal{Y}} \left(\int_{[0,1]^N} \psi(y, r) dr \right) \sigma^2(y, \Psi(y)) dy.$$

Furthermore,

$$(C.9) \quad \begin{aligned} \int_{[0,1]^N} \psi(y, r) dr &= \sum_{k \in \mathbb{Z}^N} \int_{[0,1]^N} G^2(y, k - r) dr \\ &= \int_{\mathbb{R}^N} G^2(y, r) dr =: H(y). \end{aligned}$$

By Parseval's theorem and (5.22),

$$(C.10) \quad \begin{aligned} \int_{\mathbb{R}^N} G^2(y, r) dr &= (2\pi)^{-N} \int_{\mathbb{R}^N} |\tilde{G}(y, \hat{\mu})|^2 d\hat{\mu} \\ &= (2\pi)^{-N} \int_{\mathbb{R}^N} |a_2(y, \hat{\mu}) \tilde{\varphi}(\hat{\mu})|^2 d\hat{\mu}, \end{aligned}$$

where $\tilde{G}(y, \hat{\mu})$ denotes the N -dimensional Fourier transform of $G(y, r)$ with respect to r . Returning the dependence on x_0 , we get using Assumption 2.8(2)

$$(C.11) \quad \lim_{\epsilon \rightarrow 0} D_\epsilon = \int_{\mathcal{Y}} H(x_0, y) \sigma^2(y, \Psi(x_0, y)) dy > 0.$$

Consider now the numerator in (7.5). Using (2.10), (5.23), and (7.3), we obtain after simple calculations:

$$(C.12) \quad \kappa_\epsilon^3 \sum_{z_k \in \mathcal{Z}} |G(y_j, k - b_j) + R_{j,k}|^3 \mathbb{E} |\eta_{j,k}|^3 = o(\epsilon^{n-N}),$$

where the small- o is uniform with respect to j . Then the numerator in (7.5) is bounded by

$$(C.13) \quad \sum_{y_j \in \mathcal{Y}} o(\epsilon^{n-N}) = o(1).$$

Together with (C.11) this proves Lemma 7.2.

APPENDIX D. PROOF OF (C.8)

Let D'_ϵ denote the first term on the right in (C.6). We can write D'_ϵ in the following form

$$(D.1) \quad \begin{aligned} D'_\epsilon &= \epsilon_y^{n-N} \sum_{y_j \in \mathcal{Y}} g(y_j, \partial_x \Psi(y_j) \cdot \tilde{x} + (\Psi(y_j)/\epsilon)), \\ g(y, r) &:= \psi(y, r) \sigma^2(y, \Psi(y)), \end{aligned}$$

cf. the definition of b_j in (7.2). By (C.5), $g(y, r) = g(y, r + m)$ for any $y \in \mathcal{Y}$, $r \in \mathbb{R}^N$, and $m \in \mathbb{Z}^N$.

The proof of (C.8) is done in two steps. In section D.1 we prove several auxiliary results related to the uniform distribution property of a collection of points. The final calculation of the limit then follows easily and this is done in section D.2.

D.1. Step I: using the uniform distribution property. Given two vectors $a, b \in \mathbb{R}^N$ such that $a_l < b_l$, $1 \leq l \leq N$, we define the hyperrectangle $[a, b] := [a_1, b_1] \times \cdots \times [a_N, b_N]$. Recall that $e(t) = \exp(2\pi it)$, $t \in \mathbb{R}$.

Theorem D.1. *Let $U \subset \mathbb{R}^{n-N}$ be a bounded domain and $g \in C^2(\mathbb{R}^N)$ be a function, which satisfies $g(r) = g(r + m)$ for any $r \in \mathbb{R}^N$ and $m \in \mathbb{Z}^N$. Suppose the points $v_j(\epsilon) \in \mathbb{R}^N$, $j \in \mathbb{Z}^{n-N}$, $\epsilon j \in U$, $0 < \epsilon \ll 1$, have the property*

$$(D.2) \quad \lim_{\epsilon \rightarrow 0} \epsilon^N \sum_{\epsilon j \in U} e(m \cdot v_j(\epsilon)) = 0$$

for any $m \in \mathbb{Z}^N \setminus 0$. Then

$$(D.3) \quad \lim_{\epsilon \rightarrow 0} \epsilon^N \sum_{\epsilon j \in U} g(v_j(\epsilon)) = |U| \int_{[0,1]^N} g(r) dr.$$

Theorem D.1 is well-known in the literature (see [29, Theorems 6.1, 6.2]). Usually such a result is proven for a sequence of points v_j , $j \geq 1$. We modify the statement to allow for the points in the sequence, $v_j(\epsilon)$, to depend on $\epsilon > 0$. Nevertheless, the proof in this slightly more general case is the same and based on expanding g in the Fourier series.

Let $\langle r \rangle$ denote the distance from $r \in \mathbb{R}$ to the nearest integer. We also denote $f'_l := \partial_{y_l} f(y)$, the partial derivative of f with respect to the l -th coordinate of y .

Lemma D.2. *Given a hyperrectangle $[a, b] \subset \mathbb{R}^N$, consider a real-valued $f \in C^2([a, b])$ such that*

$$(D.4) \quad \langle f'_l(y) \rangle \geq \delta, \quad y \in [a, b],$$

for some $\delta > 0$ and for some $l = l_0$, $1 \leq l_0 \leq N$. Then

$$(D.5) \quad I_\epsilon := \epsilon^N \sum_{\epsilon j \in [a, b]} e(f(\epsilon j)/\epsilon) = O(\epsilon^{1/3}), \quad \epsilon \rightarrow 0.$$

Proof. Partition $[a, b]$ into hypercubes with side length $\epsilon^{2/3}$:

$$(D.6) \quad \begin{aligned} \Delta_k &:= [y_k, y_{k+\vec{1}}], \quad y_k := a + k\epsilon^{2/3}, \\ k &= (k_1, \dots, k_N), \quad 0 \leq k_l < (b_l - a_l)\epsilon^{-2/3}, \end{aligned}$$

where $\vec{1} := (1, \dots, 1) \in \mathbb{R}^N$. To clarify, $y_k \in \mathbb{R}^N$ are points, and the l -th coordinate of y_k is denoted $y_{k,l}$. First, we show that

$$(D.7) \quad \begin{aligned} I_\epsilon(k) &:= \epsilon^{N/3} \left| \sum_{\epsilon j \in \Delta_k} e\left(\frac{f(\epsilon j)}{\epsilon}\right) - \sum_{\epsilon j \in \Delta_k} e\left(\frac{f(y_k) + f'(y_k)(\epsilon j - y_k)}{\epsilon}\right) \right| \rightarrow 0, \\ \epsilon &\rightarrow 0, \quad \Delta_k \subset [a, b]. \end{aligned}$$

Since

$$(D.8) \quad f(\epsilon j) = f(y_k) + f'(y_k)(\epsilon j - y_k) + O(\epsilon^{4/3}), \quad \epsilon j \in \Delta_k \subset [a, b],$$

it follows from (D.7)

$$(D.9) \quad I_\epsilon(k) \leq \epsilon^{N/3} \sum_{\epsilon j \in \Delta_k} \left| e(O(\epsilon^{1/3})) - 1 \right| = O(\epsilon^{1/3}), \quad \Delta_k \subset [a, b].$$

The big- O terms in (D.8), (D.9) are uniform in k since $\max_{y \in [a,b]} \|\partial_y^2 f(y)\| < \infty$. Here $\|\cdot\|$ denotes any matrix norm.

To prove (D.5), partition the sum and use (D.7), (D.9) to obtain the estimate:

$$\begin{aligned}
(D.10) \quad |I_\epsilon| &\leq \epsilon^N \sum_k \left| \sum_{\epsilon j \in \Delta_k} e \left(\frac{f(y_k) + f'(y_k)(\epsilon j - y_k)}{\epsilon} \right) \right| + O(\epsilon^{1/3}) \\
&= \epsilon^{2N/3} \sum_k \prod_{l=1}^N \left| \epsilon^{1/3} \sum_{\epsilon j_l \in [y_{k,l}, y_{k+1,l}]} e(f'_l(y_k) j_l) \right| + O(\epsilon^{1/3}).
\end{aligned}$$

Here and below

$$(D.11) \quad \sum_k := \sum_{k_1=0}^{(b_1-a_1)\epsilon^{-2/3}-1} \cdots \sum_{k_N=0}^{(b_N-a_N)\epsilon^{-2/3}-1}.$$

Next, we use the inequality

$$(D.12) \quad \left| \sum_{n=1}^J e(rn) \right| \leq \min(J, (2\langle r \rangle)^{-1}).$$

By (D.4), $\langle f'_l(y_k) \rangle \geq \delta$, $l = l_0$. Using (D.12) in (D.10) with

$$(D.13) \quad r = f'_l(y_k), \quad J = O(\epsilon^{-1/3}), \quad l = l_0,$$

gives

$$(D.14) \quad \epsilon^{1/3} \left| \sum_{\epsilon j_l \in [y_{k,l}, y_{k+1,l}]} e(f'_l(y_k) j_l) \right| \leq c \min(1, \epsilon^{1/3}/(2\delta)), \quad l = l_0.$$

Recall that $y_{k,l}$ is the l -th coordinate of y_k . Multiply both sides of (D.14) with all the remaining factors ($l \neq l_0$) in (D.10), use that all these factors are bounded, sum the resulting inequalities over k as in (D.11), and multiply by $\epsilon^{2N/3}$. This gives the same upper bound as in (D.14). Hence $I_\epsilon = O(\epsilon^{1/3})$ and the lemma is proven. \square

Corollary D.3. *Given a bounded domain $U \subset \mathbb{R}^N$, pick a real-valued $f \in C^2(U)$. Suppose for every $u \in \mathbb{Z}^N$ and every $\delta > 0$ sufficiently small, there exist $p > 0$ and a finite collection of cubes $\mathcal{B}_l \subset \mathbb{R}^n$ such that*

$$(D.15) \quad \{y \in U : |f'(y) - u| \leq p\} \subset \cup_l \mathcal{B}_l, \quad \sum_l \text{Vol}(\mathcal{B}_l) \leq \delta.$$

Then

$$(D.16) \quad \epsilon^N \sum_{\epsilon j \in U} e(f(\epsilon j)/\epsilon) \rightarrow 0, \quad \epsilon \rightarrow 0.$$

Proof. Pick $\delta > 0$ arbitrarily small. Since the set $f'(y)$, $y \in U$, is bounded, there are finitely many $u \in \mathbb{Z}^N \cap f'(U)$. Therefore, by the assumptions of the corollary, there exist $p > 0$ and a finite collection of cubes \mathcal{B}_l such that

$$(D.17) \quad \{y \in U : |f'(y) - u| \leq p \text{ for some } u \in \mathbb{Z}^N\} \subset \cup_l \mathcal{B}_l, \quad \sum_l \text{Vol}(\mathcal{B}_l) \leq \delta.$$

Denote $U(\delta) := U \setminus \cup_l \mathcal{B}_l$. By construction,

$$(D.18) \quad U(\delta) \subset \{y \in U : |f'(y) - u| > p, \forall u \in \mathbb{Z}^N\}.$$

Approximate $U(\delta)$ by a union of finitely many pairwise nonintersecting cubes Δ_l :

$$\cup_l \Delta_l \subset U(\delta), \quad \text{Vol}(U(\delta) \setminus \cup_l \Delta_l) < \delta.$$

By construction, $f(y)$ satisfies the assumptions of Lemma D.2 on each of the Δ_l . This follows from (D.18) and because $|f'(y) - u| > p$ implies that $|\partial_{y_\iota} f(y) - u_\iota| > p/N^{1/2}$ for at least one $\iota = 1, 2, \dots, N$. By Lemma D.2,

$$(D.19) \quad \epsilon^N \sum_{\epsilon j \in \Delta_l} e(f(\epsilon j)/\epsilon) \rightarrow 0, \quad \epsilon \rightarrow 0,$$

for each Δ_l , and there are finitely many of them. By choosing $\delta > 0$ small, $\cup_l \Delta_l$ can be as close to U as we like, and the desired assertion follows. \square

In what follows we apply Corollary D.3 with N replaced by $n - N$ (i.e., $U \subset \mathbb{R}^{n-N}$) and ϵ replaced by ϵ_y .

Corollary D.4. *Fix a bounded domain $U \subset \mathbb{R}^{n-N}$ and a C^2 function $\Psi : U \rightarrow \mathbb{R}^N$. Let $g \in C^2(\mathbb{R}^N)$ be a function, which satisfies $g(r) = g(r + m)$ for any $r \in \mathbb{R}^N$ and $m \in \mathbb{Z}^N$. Suppose the function $m \cdot \Psi(y) : U \rightarrow \mathbb{R}$ satisfies the assumptions of Corollary D.3 for any $m \in \mathbb{Z}^N \setminus 0$. Then*

$$(D.20) \quad \lim_{\epsilon_y \rightarrow 0} \epsilon_y^{n-N} \sum_{\epsilon_y j \in U} g(\Psi(\epsilon_y j)/\epsilon_y) = \text{Vol}(U) \int_{[0,1]^N} g(r) dr.$$

Proof. By setting $f(y) := m \cdot \Psi(y) : U \rightarrow \mathbb{R}$, Corollary D.3 implies that

$$(D.21) \quad \lim_{\epsilon_y \rightarrow 0} \epsilon_y^{n-N} \sum_{\epsilon_y j \in U} e(m \cdot \Psi(\epsilon_y j)/\epsilon_y) = 0, \quad \forall m \in \mathbb{Z}^N \setminus 0.$$

The desired result follows from Theorem D.1 by setting $v_j(\epsilon_y) = \Psi(\epsilon_y j)/\epsilon_y$. \square

D.2. Step II: computing $\lim_{\epsilon \rightarrow 0} D_\epsilon$. Fix some $0 < \delta \ll 1$ and partition \mathcal{Y} into $L(\delta)$ domains U_l , $l = 1, \dots, L(\delta)$, such that the diameter of each domain does not exceed δ . Pick any $\tilde{y}_l \in U_l$ for each l . Clearly,

$$(D.22) \quad D_\epsilon = \sum_{l=1}^{L(\delta)} \text{Vol}(U_l) \left[\frac{\epsilon_y^{n-N}}{\text{Vol}(U_l)} \sum_{y_j \in U_l} g(\tilde{y}_l, \Psi(y_j)/\epsilon_y) \right] + O(\delta).$$

Applying Corollary D.4 to each expression in brackets (i.e., with U replaced by U_l) we obtain

$$(D.23) \quad \lim_{\epsilon \rightarrow 0} D_\epsilon = \sum_{l=1}^{L(\delta)} \text{Vol}(U_l) \int_{[0,1]^N} g(\tilde{y}_l, r) dr + O(\delta).$$

By Lemma 7.1, Corollary D.4 does apply. Indeed, for Corollary D.4 to apply, the main property is that for any $m \in \mathbb{Z}^N$ and $0 < \delta \ll 1$ the set

$$(D.24) \quad \{y \in U_l : |\partial_y(m \cdot \Psi(y)) - u| \leq p\}$$

is contained in a union of finitely many cubes with the total volume not exceeding δ . Lemma 7.1 proves a slightly stronger property for all of \mathcal{Y} , where instead of a vector $m \in \mathbb{Z}^N \setminus 0$ we have $\xi \in \mathbb{R}^N \setminus 0$.

Since $\delta > 0$ can be arbitrarily small, the proof is finished.

APPENDIX E. OUTLINE OF PROOF OF LEMMA 7.3

The proof of Lemma 7.3 is similar to that of Lemma 7.2, so here we only highlight key new points.

The denominator in (7.7) is $D_\epsilon^{3/2}$, where (cf. (7.6) for the definitions of $b_j^{(l)}$ and $R_{j,k}^{(l)}$)

$$(E.1) \quad D_\epsilon = \epsilon_y^{n-N} \sum_{(y_j, z_k) \in \mathcal{V}} \left[\sum_{l=1}^L \theta_l (G(y_j, k - b_j^{(l)}) + R_{j,k}^{(l)}) \right]^2 \sigma^2(y_j, \Psi(y_j)) + O(\epsilon^a), \quad a = \min(1, 2\gamma + N).$$

Here we have used the usual substitution $z_k \cong \Psi(y_j)$ (cf. (C.6), (C.7)) and (2.10). Estimating the contribution of the remainder $R_{j,k}^{(l)}$ similarly to (C.2) and passing to the limit as in (C.8) gives

$$(E.2) \quad \lim_{\epsilon \rightarrow 0} D_\epsilon = \int_{\mathcal{Y}} \int_{\mathbb{R}^N} f^2(r, y) dr \sigma^2(y, \Psi(y)) dy, \\ f(r, y) := \sum_{l=1}^L \theta_l G(y, r - \partial_x \Psi(y) \cdot \tilde{x}_l).$$

Multiplying out the sum in the definition of f , we can write

$$(E.3) \quad \lim_{\epsilon \rightarrow 0} D_\epsilon = \sum_{l_1=1}^L \sum_{l_2=1}^L \theta_{l_1} \theta_{l_2} C(\tilde{x}_{l_1} - \tilde{x}_{l_2}), \\ C(\vartheta) := \int_{\mathcal{Y}} (G \star G)(y, \partial_x \Psi(y) \cdot \vartheta) \sigma^2(y, \Psi(y)) dy, \\ (G \star G)(y, \vartheta) := \int_{\mathbb{R}^N} G(y, \vartheta + r) G(y, r) dr.$$

Observe that if $L = 1$, $\theta_1 = 1$, and $\vartheta = 0$, then (E.3) coincides with (C.8), (C.9). By (5.22),

$$(E.4) \quad f(r, y) = (2\pi)^{-N} \int_{\mathbb{R}^N} a_2(y, \hat{\mu}) \tilde{\varphi}(\hat{\mu}) \left[\sum_{l=1}^L \theta_l e^{-i\hat{\mu} \cdot \partial_x \Psi(y) \tilde{x}_l} \right] e^{i\hat{\mu} \cdot r} d\hat{\mu}.$$

Suppose the limit in (E.2) equals zero. By Assumption 2.8(2), this implies that $f(r, y) \equiv 0$ for all $r \in \mathbb{R}^N$ and $y \in V$. The set V is introduced in Assumption 2.8(2). Also, φ is compactly supported, so $\tilde{\varphi}$ is analytic and cannot be zero on an open set. Therefore

$$(E.5) \quad \sum_{l=1}^L \theta_l e^{-i\hat{\mu} \cdot \partial_x \Psi(y) \tilde{x}_l} \equiv 0, \quad \hat{\mu} \in \mathbb{R}^N, \quad y \in V.$$

Consider the vectors $e_p := \tilde{x}_{l_1} - \tilde{x}_{l_2} \in \mathbb{R}^n$, $1 \leq l_1, l_2 \leq L$, $l_1 \neq l_2$, and the sets $V_p := \{y \in V : \partial_x \Psi(y) e_p = 0\}$. Recall that the first argument of Ψ is

$x = x_0$, which we omitted for simplicity. The \tilde{x}_l are distinct, so $e_p \neq 0$ for each p . By (2.17), each set V_p has measure zero. There are finitely many V_p , so their union is not all of V . Therefore there exists $y_0 \in V \setminus (\cup V_p)$ such that $\partial_x \Psi(y_0)e_p \neq 0$ for each p . Since the union of any finite number of the proper subspaces $(\partial_x \Psi(y_0)e_p)^\perp \subset \mathbb{R}^N$ cannot be all of \mathbb{R}^N , there exists $\hat{\mu} \in \mathbb{R}^N$ such that $\hat{\mu} \cdot \partial_x \Psi(y_0)e_p \neq 0$ for any p .

In summary, there exist $y_0 \in V$ and $\hat{\mu}$ such that $s_l := \hat{\mu} \cdot \partial_x \Psi(y_0)\tilde{x}_l$, $1 \leq l \leq L$, are pairwise distinct. Replace $\hat{\mu}$ with $\lambda \hat{\mu}$ in (E.5), differentiate with respect to λ multiple times, and set $\lambda = 0$. This gives

$$(E.6) \quad \sum_{l=1}^L \theta_l s_l^p = 0, \quad p = 0, 1, \dots, L-1.$$

Since all s_l are pairwise distinct, using the properties of the Vandermonde determinant we conclude from (E.5) and (E.6) that all $\theta_l = 0$. This contradiction proves that the limit in (E.2) is not zero unless $\vec{\theta} = 0$.

An argument to show that the limit of the numerator in (7.7) is bounded is very similar to (C.12), (C.13).

REFERENCES

- [1] H. Abels. *Pseudodifferential and Singular Integral Operators: An Introduction with Applications*. De Gruyter, Berlin/Boston, 2012.
- [2] A. Abhishek, A. Katsevich, and J. W. Webber. Local reconstruction analysis of inverting the Radon transform in the plane from noisy discrete data. *arXiv*, 2403.12909:1–23 (submitted), 2024.
- [3] R. J. Adler. *The Geometry of Random Fields*. Society for Industrial and Applied Mathematics, Philadelphia, PA, 2010.
- [4] K. B. Athreya and S. N. Lahiri. *Measure theory and probability theory*. Springer, New York, NY, 2006.
- [5] S. Berg, N. Saxena, M. Shaik, and C. Pradhan. Generation of ground truth images to validate micro-CT image-processing pipelines. *The Leading Edge*, 37(6):412–420, 2018.
- [6] N. Bissantz, H. Holzmann, and K. Proksch. Confidence regions for images observed under the Radon transform. *Journal of Multivariate Analysis*, 128:86–107, 2014.
- [7] L. Cavalier. Asymptotically efficient estimation in a problem related to tomography. *Math. Methods Statist.*, 7(4):445–456 (1999), 1998.
- [8] L. Cavalier. Efficient estimation of a density in a problem of tomography. *Ann. Statist.*, 28(2):630–647, 2000.
- [9] S. S. Chhatre, H. Sahoo, S. Leonardi, K. Vidal, E. M. Braun, and P. Patel. A Blind Study of Four Digital Rock Physics Vendor Labs on Porosity, Absolute Permeability, and Primary Drainage on Tight Outcrops. *International Symposium of the Society of Core Analysts held in Vienna, Austria*, pages 1–12, 2017.
- [10] A. Dhara, Ashis Kumar Mukhopadhyay, Sudipta Dutta, M. Garg, and N. Khandelwal. A combination of shape and texture features for classification of pulmonary nodules in lung CT images. *Journal of digital imaging*, 29:466–475, 2016.
- [11] P. Dhara, Ashis Kumar Mukhopadhyay, Sudipta Saha, M. Garg, and N. Khandelwal. Differential geometry-based techniques for characterization of boundary roughness of pulmonary nodules in CT images. *International journal of computer assisted radiology and surgery*, 11:337–349, 2016.
- [12] S. E. Divel and N. J. Pelc. Accurate Image Domain Noise Insertion in CT Images. *IEEE Transactions on Medical Imaging*, 39(6):1906–1916, 2020.
- [13] K. J. Falconer. *Fractal geometry: mathematical foundations and applications*. Wiley, third edition, 2014.

- [14] A. Faridani. Sampling theory and parallel-beam tomography. In *Sampling, wavelets, and tomography*, volume 63 of *Applied and Numerical Harmonic Analysis*, pages 225–254. Birkhauser Boston, Boston, MA, 2004.
- [15] A. Faridani, K. Buglione, P. Huabsomboon, O. Iancu, and J. McGrath. Introduction to local tomography. In *Radon transforms and tomography. Contemp. Math.*, 278, pages 29–47. Amer. Math. Soc, 2001.
- [16] D. Gilbarg and N. S. Trudinger. *Elliptic Partial Differential Equations of Second Order*. Springer, Berlin, Heidelberg, 2001.
- [17] V. Guillemin and A. Pollack. *Differential Topology*. Prentice-Hall, Inc., Englewood Cliffs, NJ, 1974.
- [18] B. Hahn and A. K. Louis. Reconstruction in the three-dimensional parallel scanning geometry with application in synchrotron-based x-ray tomography. *Inverse Problems*, 28, 2012.
- [19] L. Hormander. *The Analysis of Linear Partial Differential Operators I. Distribution Theory and Fourier Analysis*. Springer-Verlag, Berlin, 2003.
- [20] A. Katsevich. Analysis of tomographic reconstruction of objects in \mathbb{R}^2 with rough edges. *arXiv*, (2312.08259 [math.NA]), 2023.
- [21] A. Katsevich. Novel resolution analysis for the Radon transform in \mathbb{R}^2 for functions with rough edges. *SIAM Journal of Mathematical Analysis*, 55:4255–4296, 2023.
- [22] A. Katsevich. Resolution analysis of inverting the generalized N -dimensional Radon transform in \mathbb{R}^n from discrete data. *Journal of Fourier Analysis and Applications*, 29, art. 6, 2023.
- [23] A. Katsevich. Resolution of 2D reconstruction of functions with nonsmooth edges from discrete Radon transform data. *SIAM Journal on Applied Mathematics*, 83(2):695–724, 2023.
- [24] A. Katsevich. Analysis of view aliasing for the generalized Radon transform in \mathbb{R}^2 . *SIAM Journal on Imaging Sciences*, 17(1):415–440, 2024.
- [25] D. Khoshnevisan. *Multiparameter Processes. An Introduction to Random Fields*. Springer-Verlag, New York, 2002.
- [26] A. P. Korostelev and A. B. Tsybakov. Optimal rates of convergence of estimates in the stochastic problem of computerized tomography. *Problems Inform. Transmission*, 27(1):73–81, 1991.
- [27] A. P. Korostelev and A. B. Tsybakov. Asymptotically minimax image reconstruction problems. In *Topics in nonparametric estimation*, pages 45–86. Amer. Math. Soc., Providence, RI, 1992.
- [28] S. G. Krantz and H. R. Parks. *The Implicit Function Theorem: History, Theory, and Applications*. 2013.
- [29] L. Kuipers and H. Niederreiter. *Uniform Distribution of Sequences*. Dover Publications, Inc., Mineola, NY, 2006.
- [30] A. K. Louis. Exact cone beam reconstruction formulae for functions and their gradients for spherical and flat detectors. *Inverse Problems*, 32, 2016.
- [31] A. K. Louis and P. Maass. Contour reconstruction in 3-D X-ray CT. *IEEE Transactions on Medical Imaging*, 12:764–769, 1993.
- [32] F. Monard, R. Nickl, and G. P. Paternain. Efficient nonparametric Bayesian inference for X-ray transforms. *Ann. Statist.*, 47(2):1113–1147, 2019.
- [33] F. Natterer. Sampling in Fan Beam Tomography. *SIAM Journal on Applied Mathematics*, 53:358–380, 1993.
- [34] V. P. Palamodov. Localization of harmonic decomposition of the Radon transform. *Inverse Problems*, 11:1025–1030, 1995.
- [35] A. Ramm and A. Katsevich. *The Radon Transform and Local Tomography*. CRC Press, Boca Raton, Florida, 1996.
- [36] N. Saxena, R. Hofmann, F. O. Alpak, and Others. References and benchmarks for pore-scale flow simulated using micro-CT images of porous media and digital rocks. *Advances in Water Resources*, 109:211–235, 2017.
- [37] N. Saxena, A. Hows, R. Hofmann, F. O. Alpak, J. Dietderich, M. Appel, J. Freeman, and H. De Jong. Rock properties from micro-CT images: Digital rock transforms for

- resolution, pore volume, and field of view. *Advances in Water Resources*, 134(February), 2019.
- [38] N. Saxena, A. Hows, R. Hofmann, O. Alpak, J. Freeman, M. Appel, and J. Dietderich. Digital rock technology for accelerated RCA and SCAL: Application envelope and required corrections. *SPWLA 60th Annual Logging Symposium 2019*, pages 1–6, 2019.
- [39] S. Siltanen, V. Kolehmainen, S. J. Rvenp, J. P. Kaipio, P. Koistinen, M. Lassas, J. Pirttil, and E. Somersalo. Statistical inversion for medical X-ray tomography with few radiographs: I. general theory. *Physics in Medicine and Biology*, 48(10):1437–1463, may 2003.
- [40] P. Stefanov. Semiclassical sampling and discretization of certain linear inverse problems. *SIAM Journal of Mathematical Analysis*, 52:5554–5597, 2020.
- [41] P. Stefanov and S. Tindel. Sampling linear inverse problems with noise. *Asymptot. Anal.*, 132(3-4):331–382, 2023.
- [42] F. Trèves. *Introduction to Pseudodifferential and Fourier Integral Operators. Volume 2: Fourier Integral Operators*. The University Series in Mathematics. Plenum, New York, 1980.
- [43] S. Vänskä, M. Lassas, and S. Siltanen. Statistical X-ray tomography using empirical Besov priors. *Int. J. Tomogr. Stat.*, 11(S09):3–32, 2009.
- [44] A. Wunderlich and F. Noo. Image covariance and lesion detectability in direct fan-beam X-ray computed tomography. *Physics in Medicine and Biology*, 53(10):2471–2493, 2008.